International Journal of Nanomedicine

Dovepress

open access to scientific and medical research

Open Access Full Text Article

ORIGINAL RESEARCH

In vitro–in vivo evaluation of chitosan-PLGA nanoparticles for potentiated gastric retention and anti-ulcer activity of diosmin

This article was published in the following Dove Press journal:
International Journal of Nanomedicine

Walaa Ebrahim Abd El Hady
Elham Abdelmonem Mohamed
Osama Abd El-Aazeem Soliman
Hassan Mohamed EL-Sabbagh

Department of Pharmaceutics, Faculty of Pharmacy, Mansoura University, Mansoura 35516, Egypt

Background: Diosmin showed poor water solubility and low bioavailability. Poly(d,l-lactide-co-glycolide) (PLGA) nanoparticles were successfully used to improve the drugs solubility and bioavailability. Coating of PLGA nanoparticles with chitosan can ameliorate their gastric retention and cellular uptake.

Methodology: PLGA nanoparticles of diosmin were prepared using different drug and polymer amounts. Nanoparticles were selected based on entrapment efficiency% (EE%) and particle size measurements to be coated with chitosan. The selected nanoparticles either uncoated or coated were evaluated regarding morphology, ζ-potential, solid-state characterization, in vitro release, storage stability, and mucoadhesion. The anti-ulcer activity (AA) against ethanol-induced ulcer in rats was assessed through macroscopical evaluation, histopathological examination, immunohistochemical localization of nuclear factor kappa-light-chain-enhancer of activated B cells (NF-κB) and transmission electron microscopic examination of gastric tissues compared to free diosmin (100 mg/kg) and positive control.

Results: Based on EE% and particle size measurements, the selected nanoparticles, either uncoated or coated with 0.1% w/v chitosan, were based on 1:15 drug-PLGA weight ratio and 20 mg diosmin employing methylene chloride as an organic phase. Examination by scanning electron microscopy (SEM) and transmission electron microscopy (TEM) revealed nanoscopic spherical particles. Drug encapsulation within the selected nanoparticles was suggested by Fourier transform-infrared, differential scanning calorimetry (DSC) and X-ray diffractometry results. Chitosan-coated nanoparticles were more stable against size enlargement probably due to the higher ζ-potential. Only coated nanoparticles showed gastric retention as revealed by SEM examination of stomach and duodenum. The superior AA of coated nanoparticles was confirmed by significant reduction in average mucosal damage, the majority of histopathological changes and NF-κB expression in gastric tissue when compared to positive control, diosmin and uncoated nanoparticles as well as insignificant difference relative to normal control. Coated nanoparticles preserved the normal ultrastructure of the gastric mucosa as revealed by TEM examination.

Conclusion: The optimized chitosan-coated PLGA nanoparticles can be represented as a potential oral drug delivery system of diosmin.

Keywords: diosmin, poly(d,l-lactide-co-glycolide), chitosan-coating, polymeric nanoparticles, gastric retention, anti-ulcer activity

Correspondence: Elham Abdelmonem Mohamed
Department of Pharmaceutics, Faculty of Pharmacy, Mansoura University, Gomhoreyah St., Mansoura 35516, Egypt
Tel +20 106 569 0987
Fax +20 50 224 7496
Email elham.mabdelmonem@gmail.com

Introduction

There are some endogenous aggressive factors that can cause gastric ulcer such as overproduction of hydrochloric acid and pepsin, leukotrienes, refluxed bile, and stress oxygen species.[1] The defensive endogenous mechanisms against the damage

of the gastric mucosa include the surface mucus, the regulation of gastric mucosal blood flow, bicarbonate, antioxidants, surface active phospholipids, the acceleration of epithelial regeneration, and the preservation of epithelial hemostasis. Excessive gastric acid secretion was considered to be the major reason of the gastric ulcer for decades; thus, anti-cholinergic drugs, antacids, histamine H_2-receptor antagonists, and proton pump inhibitors were the main therapy regimens. Nevertheless, the limited efficacy and the adverse effects of most of the current therapies limited their application.[2] Therefore, there is a great necessity for safe and effective anti-ulcer agents.

Diosmin (3,5,7-trihydroxy-4-methoxyflavone 7-rutinoside) is a natural flavonoid glycoside that can be obtained from different plant sources or derived from the flavonoid hesperidin.[3] Diosmin has been widely used as a vascular protector for the treatment of hemorrhoids and venous leg ulcers.[4] It also exhibited anti-inflammatory, free-radical scavenging,[5] and anti-ulcer activities.[6] This drug showed gastro-protection against ethanol-induced gastric ulcer in rats by inhibiting the mitochondrial damage and MMP-9 upregulation.[7] However, diosmin is poorly soluble, thus low dissolution rate and impaired gastrointestinal absorption were observed.[8] Following oral administration, diosmin is quickly hydrolyzed by enzymes produced by intestinal microflora into its aglycone diosmetin that is absorbed through the intestinal wall to be then enzymatically esterified to its metabolite of 3,7-O-diglucuronide.[8] Consequently, a large oral dose (500 mg twice daily) is usually required.[9] However, the amount of diosmetin detected in plasma after a single oral administration of diosmin is low and highly inconsistent. The variability of absorption could be reduced by adherence to the gastrointestinal wall to allow a rapid replenishment of the absorbed drug. Small particles tend to adhere well to the mucus layer and then penetrate this layer to bind to the underlying epithelium.[10] It has been reported that oral administration of diosmin in micronized form can ameliorate its plasma concentrations due to the larger surface area and subsequent improved intestinal absorption.[11] Different strategies have been attempted to improve diosmin solubility, such as complexation with β-cyclodextrin,[6] as well as particle size reduction by formulation into nanosuspension with hydroxypropyl methylcellulose[9] and electrospinning to nanofibers.[5]

Poly(d,l-lactide-co-glycolide) (PLGA) is a synthetic copolymer that has been approved by FDA for various medical and pharmaceutical applications including drug delivery.[12] PLGA is biocompatible and biodegradable since it is hydrolyzed into non-toxic oligomer and monomer of lactic and glycolic acids that are hydrophilic and finally eliminated as carbon dioxide and water.[13,14] In addition, the degradation rate of this copolymer can be modified by controlling the molar ratios of lactic and glycolic acids in the polymer chain and the degree of crystallinity, as well as the molecular weight and stereochemistry of the polyester.[15] PLGA nanoparticles can increase the drug penetration across the different biological barriers, such as the blood–brain barrier, gastrointestinal mucosa, nasal mucosa, and ocular tissue.[16] Therefore, this copolymer has been extensively used as nanoparticulate drug delivery system to enhance the biological activity, water solubility, and bioavailability of drugs.[13] PLGA produces negatively charged, smooth surfaced, and spherical particles that are relatively resistant to salt- and pH-induced instability, and can slowly release the entrapped drugs by polymer hydrolysis. Yet, unsuccessful results have been observed in some cases possibly due to the lack of mucoadhesiveness and immune-stimulating factors.[17] Also, the negative surface charge of PLGA nanoparticles can hinder the interaction with the negatively charged plasmids and hence limit their intracellular uptake and the bioavailability of the loaded drugs.[18]

Chitosan is a naturally occurring linear amino polysaccharide (poly 1, 4-day-glucoamine) which can be obtained from crustacea shells, insects cuticles, and cell walls of some fungi.[19] Chitosan is an interesting biomaterial for entrapment of bioactive materials in nanoparticulate delivery systems due to its water solubility under acidic conditions, biocompatibility, non-toxicity as well as its mucoadhesive and permeability-enhancing properties.[18–20] Modification of PLGA nanoparticles surface with a mucoadhesive polymer, such as chitosan, can offer several advantages. Among these, increased stability of macromolecules such as proteins, providing a positive surface charge that can promote cellular adhesion and delivery system retention at the target site, as well as conjugating targeting ligands to chitosan free amine groups.[21] Mucoadhesive delivery systems increase the residence time of dosage forms at the delivery site which may lead to improved bioavailability, lower drug dose, less dosing frequency, and minimal side effects.[22] The successful use of chitosan-based gastrointestinal mucoadhesive delivery systems has been reported in some studies.[18,23] Longer residence time in the stomach is advantageous in the treatment of gastric ulcer.[24]

Therefore in this study, it was worth to prepare, characterize, and optimize polymeric nanoparticulate delivery systems of diosmin with the biodegradable and biocompatible PLGA. Coating of the selected PLGA nanoparticles with chitosan was attempted and its effects on the gastric retention of diosmin were assessed. Additionally, the effects of the selected PLGA nanoparticles either uncoated or coated on cytoprotective activity of diosmin against ethanol-induced ulcer in rats were investigated through macroscopical, histopathological, and transmission electron microscope examination of gastric tissues as well as immunohistochemical localization of gastric nuclear factor kappa-light-chain-enhancer of activated B cells (NF-κB).

Materials and methods

Materials

Diosmin was purchased from Sigma-Aldrich, St. Louis, MO, USA. PLGA (lactide–glycolide 50:50; Viscosity 0.8–1.2 dL/g) was kindly supplied by Purac Biomaterials, Holland. Chitosan (molecular weight 100,000–300,000) and polyvinyl alcohol (molecular weight 31,000–50,000 Da) were purchased from Acros organics, Belgium. Methylene chloride, dimethyl sulfoxide, and glacial acetic acid were purchased from Adwic, EL Nasr Pharmaceutical Chemicals, Co., Egypt. All other chemicals were of fine analytical grades.

Preparation of diosmin nanoparticles

The effects of several formulation parameters including drug:polymer weight ratio, loaded drug amount, and the organic phase nature on the particle size and entrapment efficiency% (EE%) of diosmin nanoparticles were studied to select PLGA nanoparticles to be coated with chitosan aiming to enhance their gastric retention and the anti-ulcer activity (AA) of diosmin. Different diosmin:PLGA weight ratios (1:10, 1:15, 1:20) were used. The loaded drug was either 10 or 20 mg. The organic solvents employed were methylene chloride and ethyl acetate individually since they are water immiscible with higher vapor pressure, and hence their removal is facilitated.[25] In addition, they are good solvents for PLGA and much less toxic than chloroform and acetonitrile.[26]

Nanoparticles were prepared according to the emulsion–solvent evaporation method.[27] Briefly, accurately weighed PLGA was dissolved in 4 mL of either methylene chloride (F1–F7) or ethyl acetate (F8–F13) (Table 1). Diosmin was dissolved in 1 mL dimethylsulfoxide. The resulting organic solutions were vortexed (Model VM-300, Gemmy Industrial Corp, Taipei, Taiwan). The organic phase was then poured into 30 mL aqueous phase containing 2% w/v polyvinyl alcohol with ultrasonic homogenization (Ultrasonic homogenizer, Cole-Parmer Instrument Co., Chicago. IL, USA) at 90% amplitude for 2 mins. The organic solvent was evaporated overnight under a moderate magnetic stirring (Heidolph, IL, USA). Nanoparticles were recovered by centrifugation at 13,000 rpm (Heraeus, GmbH, Osterode, Germany) for 1 h and washed with double deionized water. The washing was performed in triplicate and then the nanoparticles were resuspended in double deionized water and lyophilized (SIM, FD8-8T, Newark, NJ, USA).

Chitosan-PLGA nanoparticles of diosmin (F14–F16) were prepared following the same procedure except that chitosan was dissolved in an aqueous solution of 0.2% v/v acetic acid at three different concentrations (0.10%, 0.15%, and 0.30% w/v) and then mixed with the aqueous solution of 2% w/v polyvinyl alcohol to obtain 30 mL aqueous phase (Table 2).[28]

Characterization of diosmin nanoparticles

Determination of entrapment efficiency%

The lyophilized nanoparticles (SIM, FD8-8T, Newark, NJ, USA) were mixed with 10 mL dimethylsulfoxide and properly diluted to be assayed spectrophotometrically at 269 nm (ultraviolet/visible [UV/VIS] spectrophotometer; JASCO, Tokyo, Japan) against a blank of the plain nanoparticles that were treated the same. The experiments were carried out in triplicate. Entrapment efficiency% (EE%) was calculated as follows:[29]

$$EE\,\% = \frac{\text{Drug weight in nanoparticles}}{\text{Weight of drug and polymer added}} \times 100\%$$

Particle size measurements

Dynamic light scattering technique (Malvern Instruments Ltd., Malvern, Worcestershire, UK) was used to evaluate the size distribution of the prepared nanoparticles. The lyophilized nanoparticles were reconstituted in double deionized water, properly diluted, and sonicated to obtain uniformly distributed particles.

Scanning electron microscopy (SEM)

The shape and surface characteristics of diosmin as well as the lyophilized uncoated and chitosan-coated PLGA nanoparticles were recorded using SEM (JSM-6510 LV; JEOL, Tokyo, Japan). Samples were mounted on metal stub using

double sided adhesive carbon tapes. Samples were coated with a gold layer and visualized under SEM at 30 kV.

Transmission electron microscopy (TEM)

The morphology of the selected uncoated and coated PLGA nanoparticles was studied using transmission electron microscope (TEM-2100, JEO, Tokyo, Japan) operated at an accelerating voltage of 160 kV. The lyophilized nanoparticles were reconstituted with double deionized water, properly diluted and sonicated for 2 mins. One drop was added on Formvar-coated copper grid (200 meshes, Science Services, Munich, Germany) and the excess material was removed with a filter paper. After the complete drying at room temperature, the image was captured and the analysis was done using imaging viewer software.

ζ-potential determination

ζ-potential of the selected uncoated and coated PLGA nanoparticles was measured using photon correlation spectroscopy-based instrument at 25°C (Malvern Instruments). ζ-potential was estimated on the basis of electrophoretic mobility under an electric field.[30] To determine nanoparticles surface charge, the lyophilized samples were reconstituted and properly diluted with double deionized water.

Solid-state characterization

Fourier transform-infrared (FT-IR) spectra, differential scanning calorimetry (DSC) curves, and X-ray diffractometry (XRD) patterns of the selected PLGA nanoparticles either uncoated or chitosan-coated were recorded in comparison with diosmin, the polymer(s), the corresponding physical mixture (PM), and the plain nanoparticles.

FT-IR spectroscopy

FT-IR spectra of samples homogeneously mixed with KBr and compressed into discs were traced in the region of 400–4000 cm^{-1} employing FT-IR spectrophotometer (Madison Instruments, Middleton, WI, USA).

Differential scanning calorimetry (DSC)

DSC thermograms were recorded using differential scanning calorimeter (model DSC-4, PerkinElmer Inc., Waltham, MA, USA). Five milligrams of each sample were separately sealed in aluminum pans. Then, they were heated at the range from 35°C to 400°C at a heating rate of 10°C/min under a constant purging of dry nitrogen at 20 mL/min. Indium with purity of 99.99% and melting point of 156.6°C was used to calibrate the temperature.

X-ray diffractometry (XRD)

XRD patterns of the examined samples were obtained using X-ray diffractometer (Diano, Woburn, MA, USA) operated at 45 kV, 9 mA, and at an angle of 2θ.

In vitro drug release study

In vitro release of diosmin from the selected uncoated and chitosan-coated PLGA nanoparticles was studied in comparison with free diosmin using USP apparatus II (paddle method) (Dissolution Apparatus USP Standards, Scientific, DA-6D, Bombay, India). A dissolution medium consisting of 500 mL borate buffer pH 10.5 was kept at 37±0.5°C and stirred at 100 rpm. Accurately weighed sample of the lyophilized nanoparticles equivalent to 20 mg diosmin were introduced into the dissolution tester cells. At predetermined time intervals (0.5, 1, 2, 3, 4, 6, 8, 24, 48, and 72 h), 3 mL of the dissolution medium was withdrawn and replaced with an equal volume of a fresh dissolution medium. The collected aliquots were filtered and spectrophotometrically analyzed for drug concentration at 269 nm (ultraviolet/visible [UV/VIS] spectrophotometer; JASCO). The blank was the corresponding plain nanoparticles that were treated the same as the medicated. Each experiment was done in triplicate and the average percentage drug released was calculated to construct in vitro release curves.

Release kinetics

First-order and zero-order kinetics[31] as well as diffusion-controlled release model[32] were applied to analyze in vitro release data. To verify the release mechanism, Korsmeyer–Peppas kinetic model ($m_t/m_\infty = kt^n$) was also used as a logarithmic relation of the fraction of drug released (m_t/m_∞) and the release time (t), where k is the kinetic constant and n is the diffusional exponent of the drug release calculated as the slope of the plot.[33] The model showing the greatest correlation coefficient (r^2) was proposed to explain the drug release mechanism from the studied nanoparticles.

Stability study

The stability of the lyophilized selected uncoated and chitosan-coated PLGA nanoparticles was evaluated during the storage period of 3 months at refrigerator (4±1°C) and room (25±1°C) temperatures. Nanoparticles were examined regarding particle size, EE%, and ζ-potential, as described above, at 0, 1, 2 and 3 months. Average drug retention (%) of the stored nanoparticles was also calculated over the storage period.

In vivo evaluation

Animals

All animal handling and procedures were performed in accordance with US National Institute of Health Guide for the Care and Use of Laboratory Animals (NIH publication No. 85–23, revised 1996). Approval of the protocol by the Ethical Committee of Faculty of Pharmacy, Mansoura University, Egypt, was accomplished. Animals were kept under regular 12 h light/12 h dark cycles at a temperature of 25±1°C and a relative humidity of 55±5%. The animals had free access to a standard laboratory food and water.

Mucoadhesion study

Thirty-six male Sprague-Dawley rats weighting 200±20 g were used to perform the mucoadhesion study. They were randomly divided into six groups of six rats each. Before the day of the experiment, all rats were fasted overnight but had free access to water. Animals of groups I and II orally received diosmin suspension in 1% w/v carboxymethylcellulose (CMC) at a dose of 100 mg/kg. The selected uncoated PLGA nanoparticles dispersion at a dose equivalent to 100 mg/kg of diosmin was orally given to rats of groups III and IV. Rats of groups V and VI orally administered chitosan-coated PLGA nanoparticles dispersion at a dose equivalent to 100 mg/kg of the drug. Oral administration was accomplished by use of feeding tube. After 2 h, animals of groups I, III, and V were euthanized under deep ether anesthesia. Euthanization under deep ether anesthesia of rats of groups II, IV, and VI was performed after 8 h. Euthanization was followed by immediate laparotomy to collect stomachs and small intestines in 2.5% (w/v) aqueous glutaraldehyde to be quickly soaked in water before freeze-drying and SEM (JSM-6510 LV; JEOL) examination.[34]

Induction of gastric ulcer and treatment protocol

Thirty male Sprague-Dawley rats (200±20 g) were randomly assigned into five groups (six rats per each). Animals of groups I (normal control) and II (positive control) did not receive any treatment for 5 days. Diosmin at a dose of 100 mg/kg displayed a protection against ethanol-induced gastric injury in rats.[7] Thus, oral pretreatment of the other three groups was continued for successive 5 days with free diosmin at a dose of 100 mg/kg (group III), uncoated PLGA nanoparticles (equivalent to 100 mg/kg of diosmin, group IV), or chitosan-coated PLGA nanoparticles (equivalent to 100 mg/kg of diosmin, group V). On the fifth day, all rats had free access to water but were deprived of food for 24 h. On the sixth day, gastric mucosal injury was induced in rats of groups II (positive control), III, IV, and V by a single intragastric instillation of 70% ethanol (10 mL/kg).[35]

Tissue collection and preparation

The rats were euthanized under deep ether anesthesia 2-h post-intragastric instillation of 70% ethanol. Immediate laparotomy was followed by stomach separation that was opened along the greater curvature and rinsed with normal saline to get rid of gastric contents and blood clots. Tissue specimens were collected from glandular and non-glandular portions of each stomach and immersed in 10% buffered formalin. All fixed specimens were routinely processed to prepare two sets of 5 µm thick paraffin-embedded sections for histopathological examination and immunohistochemical assessment of NF-κB.

Macroscopic evaluation

The gastric segments were examined by an observer who was blinded to the identity of samples. Stomachs were blotted dry and photographed to be inspected for gross gastric injury. Paul's index and AA were calculated to assess the anti-ulcer potential of diosmin either as free drug or encapsulated within PLGA or chitosan-PLGA nanoparticles.[29] Paul's index was calculated by multiplying the average ulcers number by the percentage incidence of animals with ulcers to be then divided by 100. In addition, AA was estimated by dividing Paul's index of the positive control group (II) by that of each of the treatment groups. AA was indicated if it was two units or more.[29]

Histopathological examination

Gastric tissue samples fixed in 10% (v/v) buffered formalin solution were washed then dehydrated by alcohol, cleared in xylene, and embedded in paraffin in hot air oven (56°C) for 24 h. Paraffin blocks were cut into 5 µm sections to be then stained with H&E according to a previously reported method.[36] The stained sections were examined under a light microscope (Leica Microsystems). The histopathological examination was performed by a qualified pathologist unaware of the specimens' identity in order to prevent any bias.

Gastric microscopic damage was scored based on the criteria described in the literature.[37] One centimeter segment of glandular portion of each stomach was examined for epithelial cell loss (score: 0–3), edema in submucosa (score: 0–4), congestion in submucosa (score: 0–4), and the presence of inflammatory cells (score: 0–3). Also, 1-

cm segment of non-glandular portion of each stomach was examined for submucosal edema and congestion (score: 0–4).

Immunohistochemical loclization of NF-κB

The second set of paraffin-embedded sections was used for immunohistochemical detection of NF-κB. After removal of paraffin with graded xylene followed by rehydration in ethanol, blocking of the endogenous peroxidase activity was obtained by 3% hydrogen peroxide (H_2O_2) for 5 min at room temperature. For antigen retrieval, tissue sections were put in glass jars containing 0.01 M sodium citrate buffer (pH 6.0) and boiled in a microwave oven twice for 5 mins each to enhance immunoreactivity and reserve the antigenicity that was masked by some epitopes in formalin-fixed paraffin-embedded tissues. The slides were allowed to cool and then rinsed with phosphate buffer saline pH 7.2. Immunohistochemical staining was done according to the manufacturer's instructions using ready to use primary polyclonal rabbit anti-NF-κB (Santa Cruz Biotechnology Inc., CA, USA) at a concentration of 1 µg/mL in 5% bovine serum albumin in tris-buffered saline overnight at 4°C. The slides were then washed with tris-buffered saline and incubated with secondary anti-rabbit IgG using Vector Elite ABC kit (Vector Laboratories, Burlingame, CA, USA). Finally, the sections were washed with tris-buffered saline and the immunoreaction was visualized using 3,3-diaminobenzidine tetrahydrochloride (Substrate Kit, Vector Laboratories Inc., CA, USA). Sections were washed under running tap water for 10 mins, and then counterstained with Mayer's hematoxylin. Intensity of positively stained cells was evaluated using a digital camera (Olympus Corporation, Tokyo, Japan) placed on a light microscope (Leica Microsystems, Wetzlar, Germany). The intensity of immunohistochemical staining was scored as follows: 0, negative; 1, weak; 2, moderate; and 3, strong staining. All readings were blindly performed by a pathologist.

TEM examination of ultrastructure of the gastric mucosa

Gastric specimens (2 mm×2 mm) close to the gastric antrum were fixed in 2.5% glutaraldehyde prepared in phosphate buffer at room temperature. After 2 h, the samples were postfixed in 1% osmium tetroxide prepared in phosphate buffer for 1 h. Samples were washed with buffer, dehydrated in gradual ethanol (30–100°), and finally embedded in epoxypropyl ether of glycerol (EPON 812, Carl Roth GmbH, Karlsruhe, Germany). Ultrathin sections were contrasted with saturated uranyl acetate and lead citrate to be examined under TEM.

Statistical analysis

Statistical analysis using one-way ANOVA, followed by Tukey–Kramer multiple comparisons test was carried out employing GraphPad Prism version 5.00 (GraphPad software, San Diego, CA, USA). The results were statistically analyzed at the significance levels of $P<0.05$, <0.01, and <0.001.

Results and discussion

Characterization of diosmin nanoparticles

Entrapment efficiency% (EE%)

The results indicated that drug:polymer weight ratio, loaded drug amount and the organic phase nature affected EE% of uncoated diosmin-PLGA nanoparticles (F1-F13, Table 1). At the same drug-loaded amount (10 or 20 mg), the increase in the polymer content from 1:10 to 1:15 drug:polymer weight ratio resulted in a rise in EE%. This behavior was more pronounced on the use of methylene chloride (F1–F7) rather than ethyl acetate (F8–F13) as organic phase. The increase in the polymer concentration could cause an elevation of the organic phase viscosity providing more resistance against the drug diffusion from the organic phase to the aqueous phase as well as the expected faster polymer precipitation might allow less time for drug molecules to diffuse out of nanoparticles.[38] Similarly, as the initial drug concentration in the organic phase especially methylene chloride increases from 10 mg (F1–F3) to 20 mg (F4–F6) keeping the drug:polymer weight ratio constant either 1:10, 1:15 or 1:20, the drug entrapment increased. The increase in the concentration of either drug or polymer could result in more drug–polymer interaction promoting the drug encapsulation.[38] Surprisingly, a further increase in the concentration of either the polymer to 1:20 (F3 and F6) compared to 1:15 (F2 and F5, respectively) or diosmin (30 mg, F7) relative to the corresponding based on 20 mg (F4) caused a decrease in EE%. These results may be attributed to reaching the limit of drug miscibility in the polymer beyond which no increase in the drug entrapment occurs possibly due to the attraction of free drug molecules within the polymer matrix toward those in the aqueous phase.[39] Thus, it can be said that the limit of drug miscibility in the polymer was attained at drug:polymer weight ratio of 1:15 and loaded drug amount of 20 mg.

Table 1 Characterization of the uncoated PLGA nanoparticles

Formula code	Drug:polymer (mg)	Size (nm)	PDI	EE%
F1	10:100	594.40±13.40	0.21±0.02	31.40±3.60
F2	10:150	552.90±18.40	0.16±0.08	50.90±4.80
F3	10:200	165.80±3.30	0.37±0.10	48.50±3.90
F4	20:200	303.10±49.80	0.19±0.03	70.90±5.30
F5	20:300	155.90±3.10	0.20±0.15	75.30±2.60
F6	20:400	133.50±0.20	0.28±0.10	58.60±1.90
F7	30:300	259.10±5.20	0.53±0.01	66.95±3.11
F8	10:100	482.50±2.50	0.33±0.00	48.40±4.30
F9	10:150	432.00±8.71	0.33±0.01	49.60±3.20
F10	10:200	404.30±7.50	0.22±0.00	37.00±2.16
F11	20:200	545.30±15.60	0.20±0.05	49.40±1.40
F12	20:300	450.40±5.30	0.31±0.29	55.60±0.30
F13	20:400	340.20±17.20	0.17±0.14	40.10±2.20

Notes: Data are expressed as mean±SD (n=3); F1–F7, uncoated PLGA nanoparticles prepared using methylene chloride; F8–F13, uncoated PLGA nanoparticles prepared using ethyl acetate.
Abbreviations: PLGA, poly(d,l-lactide-co-glycolide); PDI, poly dispersity index; EE%, entrapment efficiency%.

Use of methylene chloride as organic solvent imparted higher EE% at the same drug:polymer weight ratio, particularly when the loaded drug amount was 20 mg (F4–F6), in comparison with ethyl acetate (F11–F13). The higher water miscibility of ethyl acetate (8.70%) than methylene chloride (1.32%) and the expected faster partitioning in the aqueous phase and polymer precipitation in ethyl acetate could diminish the drug incorporation into PLGA nanoparticles.[40]

At drug:polymer weight ratio of 20:300 (F5), the highest EE% was obtained, and hence diminished material loss, improved particle production, and lower manufacturing cost can be expected.[41] Therefore, F5 was selected to be coated with chitosan at different concentrations (0.10%, 0.15%, and 0.30% w/v) and further investigated (Table 2). Those coated with 0.10% w/v chitosan (F14) showed mean EE% of 67.40 ±2.90% that insignificantly changed on the increase in chitosan concentration to 0.15 w/v (F15) or 0.30% w/v (F16) since chitosan concentration was much smaller than PLGA, and hence it might have not affected the organic phase viscosity and drug diffusion to the aqueous phase (Table 2). Thus, 0.10% w/v chitosan-coated nanoparticles containing 20:300 drug-PLGA (F14) using methylene chloride was further examined compared to the corresponding uncoated PLGA nanoparticles (F5) and the free drug.

Particle size analysis

Average diameter of ≤594.4±13.40 nm and PDI values ≤0.53±0.01, suggesting narrow size distribution, were recorded. The effects of drug:polymer weight ratio and the organic phase nature on the particle size of the uncoated nanoparticles were investigated (Table 1).

A significant (P<0.05) lowering in the average size was observed on the increase in the polymer concentration. Higher polymer concentration may have resulted in increased viscosity of the organic phase which might have counteracted the diffusion and Ostwald ripening, so smaller particles were obtained.[42] Ostwald ripening does not depend on particles coalescence but on their diffusive transport through the dispersion medium.[42]

Ethyl acetate is partially water-miscible, while methylene chloride is immiscible with water.[43] Some authors claimed that smaller particles are obtained with less water-miscible organic solvents such as methylene chloride that was at the top of the list of such solvents.[25] This may explain the smaller average

Table 2 Characterization of chitosan-coated PLGA nanoparticles

Formula code	Drug:polymer (mg)	Size (nm)	PDI	EE%	ζ-potential (mV)
F14	20:300	337.60±41.00	0.30±0.09	67.40±2.90	+27.40±2.90
F15	20:300	539.50±4.60	0.22±0.01	64.20±1.30	+28.80±2.70
F16	20:300	862.00±18.07	0.24±0.01	62.30±2.10	+33.00±2.50

Notes: Data are expressed as mean±SD (n=3). F14, F15, and F16 were the selected PLGA nanoparticles (F5) coated with 0.10%, 0.15%, and 0.30% w/v chitosan, respectively.
Abbreviations: PLGA, poly(d,l-lactide-co-glycolide); PDI, poly dispersity index; EE%, entrapment efficiency%.

size of the majority of nanoparticles prepared using methylene chloride (F3–F7) rather than ethyl acetate (F8–F13). At high polymer concentration (≥200 mg), the effect of the enhanced viscosity of methylene chloride (F3–F7) predominated due to the higher solubility of PLGA in this solvent relative to ethyl acetate. Thus, the slower drug diffusion may have counteracted Ostwald ripening, and hence smaller nanoparticles were formed.[42]

As illustrated in Table 2, a distinct increase in the mean diameter of the selected uncoated PLGA nanoparticles (F5) was observed on coating with chitosan at the three concentrations employed (F14–F16). This may be explained on the basis that the protonated amino groups of chitosan may enable intermolecular hydrogen bonding with carboxylic groups of PLGA allowing chitosan adsorption on PLGA surface.[28] The smallest particle size was seen with the lowest chitosan concentration (0.10% w/v, F14). Consequently, this formulation was further studied in comparison with that based on PLGA only (F5).

SEM examination

The free drug appeared as irregular microparticles with wide size distribution (Figure 1A). On the other hand, uncoated and coated nanoparticles were nanometric with narrower size distribution being nearly spherical with smooth surface (Figure 1B and C, respectively). Spherical particles may offer the maximum volume for drug incorporation.[44] Selective accumulation in inflamed ulcerative tissues, improved cell uptake, and hence reduced dose and subsequent cost-effectiveness can be expected.[28]

TEM examination

In agreement with SEM results, TEM images exhibited spherical nanoscopic uncoated (F5) and chitosan-coated (F14) nanoparticles (Figure 2). In case of the coated nanoparticles, a solid dense polymer core surrounded by evenly distributed coat of chitosan appeared. In accordance with particle size measurements, uncoated nanoparticles possessed smaller size than those coated with chitosan. Possibility of chitosan adsorption and binding to PLGA surface via hydrogen bonding between the protonated amino groups of chitosan and carboxylic groups of PLGA may still explain these results.[28]

ζ- potential

The selected uncoated PLGA nanoparticles (F5) showed a relatively low negative ζ-potential equal to −10.50±0.20

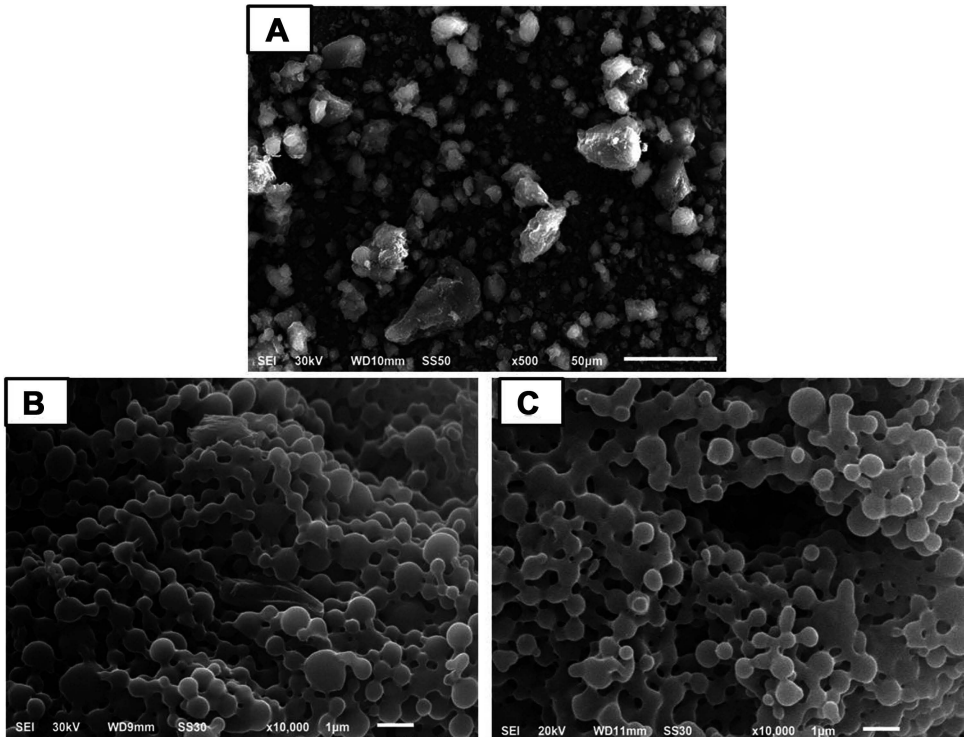

Figure 1 Scanning electron microscopy.
Notes: (**A**) Free diosmin, (**B**) uncoated diosmin-PLGA nanoparticles (F5), and (**C**) chitosan-coated PLGA nanoparticles (F14).
Abbreviation: PLGA, poly(d,l-lactide-co-glycolide).

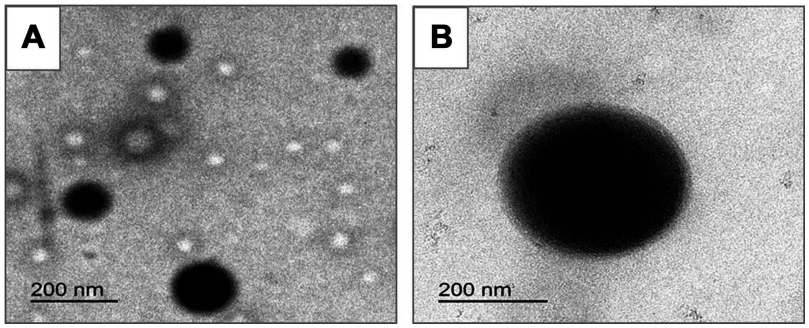

Figure 2 Transmission electron microscopy.
Notes: (**A**) Uncoated diosmin-PLGA nanoparticles (F5) and (**B**) chitosan-coated PLGA nanoparticles (F14).
Abbreviation: PLGA, poly(d,l-lactide-co-glycolide).

which could be referred to the carboxylic groups on the nanoparticles surface that were partially shielded by polyvinyl alcohol.[45] Successful coating of PLGA nanoparticles with chitosan was reflected by the higher positive ζ-potential due to the amino groups in chitosan (Table 2). This can be attributed to the intermolecular hydrogen bonding of amino groups of chitosan with carboxylic groups of PLGA allowing chitosan adsorption on PLGA surface and masking the original negative charge of PLGA carboxylic groups.[28] The increase in chitosan concentration to 0.30% w/v resulted in a significant rise in average ζ-potential possibly due to the adsorption of the subsequent layers of chitosan on the first layer.[14] The higher ζ-potential values of chitosan-coated nanoparticles than those of uncoated PLGA nanoparticles can lead to a larger repulsive force; thus, more enhanced stability against aggregation can be expected.[46]

Solid-state characterization

FT-IR

Figure 3 depicts FT-IR spectra of uncoated (A) and coated (B) nanoparticles in comparison with free diosmin, the polymer(s), the corresponding PM, and the plain nanoparticles. The characteristic peaks of diosmin at 3500 and 950 cm^{-1} were detected in its FT-IR spectrum (Figure 3A and B, I).[9] In addition, it showed absorption bands at 1660 cm^{-1} due to the aromatic ketonic carbonyl stretching (C=O vibration), as well as at 1611 and 1502 cm^{-1} assigned to the stretching of C=C bond in the aromatic ring.[3]

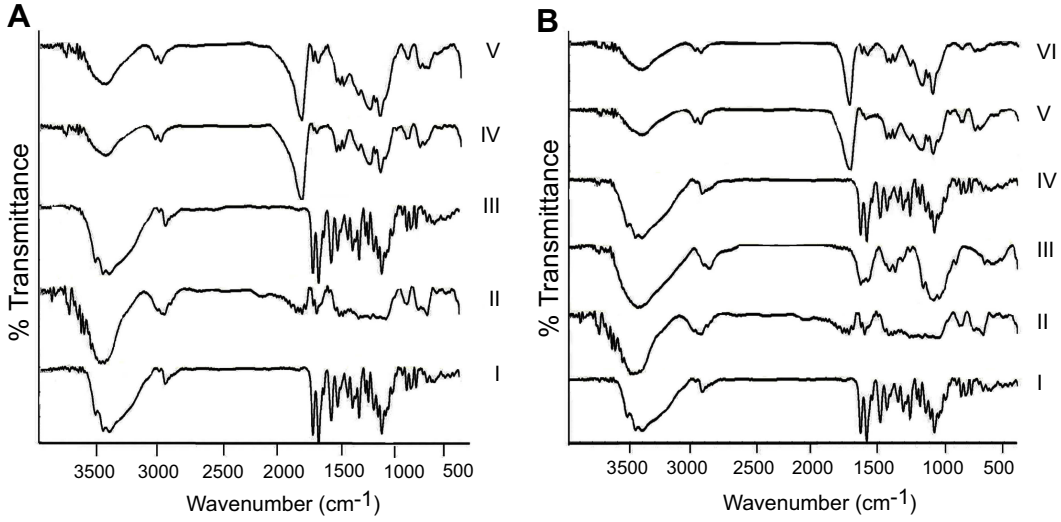

Figure 3 Fourier transform-infrared spectra.
Notes: (**A**) Uncoated diosmin-PLGA nanoparticles (F5). (I) Diosmin, (II) PLGA, (III) diosmin:PLGA 1:1 PM, (IV) plain uncoated nanoparticles, and (V) medicated uncoated PLGA nanoparticles. (**B**) Chitosan-coated PLGA nanoparticles (F14). (I) Diosmin, (II) PLGA, (III) chitosan, (IV) diosmin:chitosan 1:1 PM, (V) plain chitosan-coated nanoparticles, and (VI) medicated chitosan-coated nanoparticles.
Abbreviations: PLGA, poly(d,l-lactide-co-glycolide); PM, physical mixture.

PLGA spectrum (Figure 3A and B, II) exhibited stretching peaks of C=O at 1753 cm^{-1},[47] C–H bending at 859–1465 cm^{-1} as well as CH, CH_2, and CH_3 stretching vibration between 2885 and 3000 cm^{-1}, and finally OH stretching around 3455–3500 cm^{-1}.[48] PLGA responded at 2955 cm^{-1} due to the linear CH_2 stretching and at 1756 cm^{-1} due to the ester bond.[49] According to Figure 3B (III), the intense peaks at 1658 and 1600 cm^{-1} in chitosan spectrum confirmed the presence of amide I and amide II. Also, the peak of C–H stretch and C–H bend appeared at 2875–2900 and 1362–1426 cm^{-1}, respectively. The peak at 3449 cm^{-1} corresponding to N–H stretch was also present in chitosan spectrum. These spectral characteristics were in agreement with those reported.[19] The characteristic peaks of the drug and either polymer were present in the spectrum of the corresponding PM (Figure 3A, III and B, IV) with no additional peaks negating their interaction. The spectrum of medicated nanoparticles either uncoated (Figure 3A, V) or coated (Figure 3B, VI) was similar to that of the corresponding plain nanoparticles (Figure 3A, IV and B, V, respectively); thus, drug encapsulation within the examined nanoparticles can be suggested.

DSC

Figure 4 represents the thermal behavior of uncoated (A) and coated (B) nanoparticles in comparison with free diosmin, the polymer(s), their PM, and plain nanoparticles. DSC thermogram of free diosmin showed a sharp endothermic peak at 285.40°C indicating its melting point and its crystalline nature as well as a broad endothermic peak at 112.90°C corresponding to its dehydration (Figure 4A and B, I).[3]

In DSC curve of PLGA (Figure 4A and B, II), there was only an endothermic peak at 368.90°C reflecting its decomposition and amorphous nature.[14] In chitosan thermogram, an initial endothermic peak at 75.10°C possibly due to dehydration and higher exothermic peak at 298.80°C due to degradation were identified (Figure 4B, III).[50] The presence of characteristic peaks of diosmin and either polymer in the thermogram of their PM negated their interaction (Figure 4A, III and B, IV). PLGA endothermic peak was shifted to a lower temperature in the thermogram of its PM with diosmin possibly due to the dissolution of PLGA in the molten diosmin.[51] The thermograms of uncoated (Figure 4A, V) or coated (Figure 4B, VI) nanoparticles were similar to those describing the corresponding plain nanoparticles (Figure 4A, IV and B, V); thus, drug entrapment within the medicated nanoparticles can be suggested. Chitosan peak could not be recognized in the thermogram of the coated PLGA nanoparticles (Figure 4B, VI) probably due to the lower chitosan amount (30 mg) relative to that of PLGA (300 mg).

XRD

Figure 5 illustrates XRD patterns of free diosmin and the

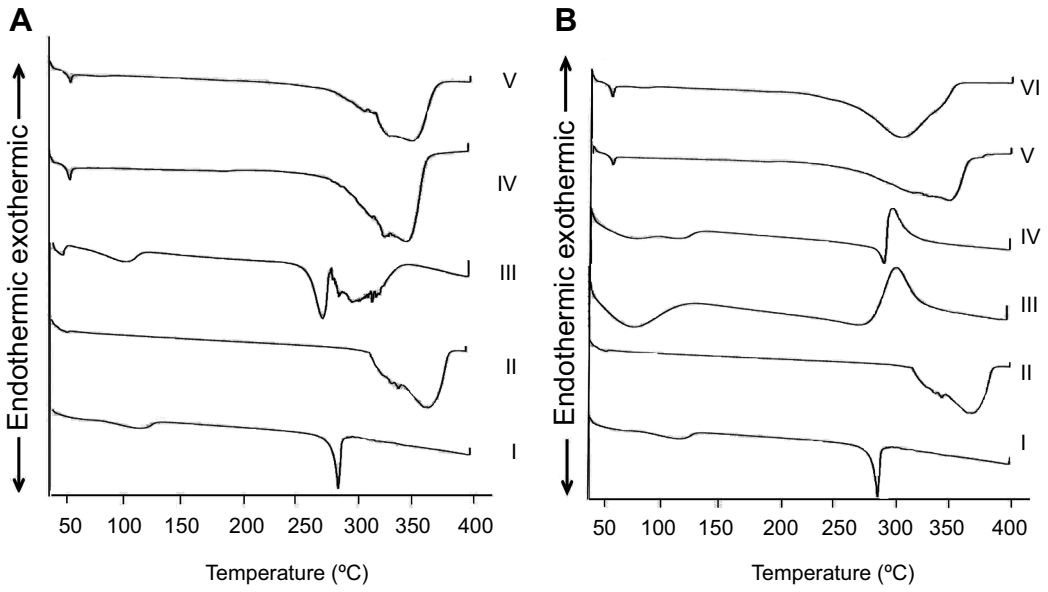

Figure 4 Differential scanning calorimetry.
Notes: (**A**) Uncoated diosmin-PLGA nanoparticles (F5). (I) Diosmin, (II) PLGA, (III) diosmin:PLGA 1:1 PM, (IV) plain uncoated nanoparticles, and (V) medicated uncoated PLGA nanoparticles. (**B**) Chitosan-coated PLGA nanoparticles (F14). (I) diosmin, (II) PLGA, (III) chitosan, (IV) diosmin:chitosan 1:1 PM, (V) plain chitosan-coated nanoparticles, and (VI) medicated chitosan-coated nanoparticles.
Abbreviations: PLGA, poly(d,l-lactide-co-glycolide); PM, physical mixture.

polymer(s) as well as the corresponding PM, plain, and medicated nanoparticles. In agreement with DSC results, diffraction pattern of diosmin showed different intense peaks at 12.24°, 13.7°, 15.63°, 19.79°, 21.43°, 22.52° and 25.00° reflecting its crystalline nature (Figure 5A and B, I).[9] The amorphous nature of both PLGA and chitosan was confirmed by the absence of diffraction peaks in their XRD diffractograms (Figure 5A, II and B, III, respectively). The interaction between diosmin and any of these polymers cannot be suggested due to the presence of drug diffraction peaks in XRD patterns of its PM with either PLGA (Figure 5A, III) or chitosan (Figure 5B, IV). On the other hand, XRD patterns of medicated nanoparticles either uncoated (Figure 5A, V) or coated (Figure 5B, VI) were similar to those of the corresponding plain nanoparticles (Figure 5A, IV and B, V, respectively) and the drug diffraction peaks were not seen. In accordance with FT-IR and DSC results, this can still indicate the drug encapsulation in the examined nanoparticles.

In vitro release study

In vitro release profiles of diosmin from uncoated (F5) and chitosan-coated nanoparticles (F14) in comparison with free drug are illustrated in Figure 6. The slow dissolution of free diosmin could be attributed to its poor wettability and consequent agglomeration.[9] The release pattern of diosmin from both types of nanoparticles was biphasic. An initial rapid release up to 8 h was followed by a sustained release phase till 72 h. Similar results were reported for PLGA nanoparticles.[52] The rapid drug release could be due to the fast dissolution of the drug adsorbed on nanoparticles surface and the enhanced surface diffusion of the release medium due to the large surface area of the nanoparticles.[53] The sustained release phase can be referred to the drug encapsulated within PLGA polymeric matrix that could be released by the slow diffusion. Coating of nanoparticles with chitosan reduced the drug release during the sustained release phase possibly due to the protection against desorption and diffusion of the drug by chitosan coat on PLGA nanoparticles.[15] The rapid release may provide the therapeutic drug concentrations that could be maintained by the sustained drug release.[28] As well, the drug sustained release may enable the reduction in the dose frequency promoting the patient satisfaction.

Release kinetics

Table 3 shows the results of kinetic analysis of diosmin release results from the uncoated and coated nanoparticles. In vitro release of diosmin from both types of nanoparticles during rapid and sustained release phases can be explained by Higuchi model suggesting diffusion-controlled drug release. Higuchi diffusion has described

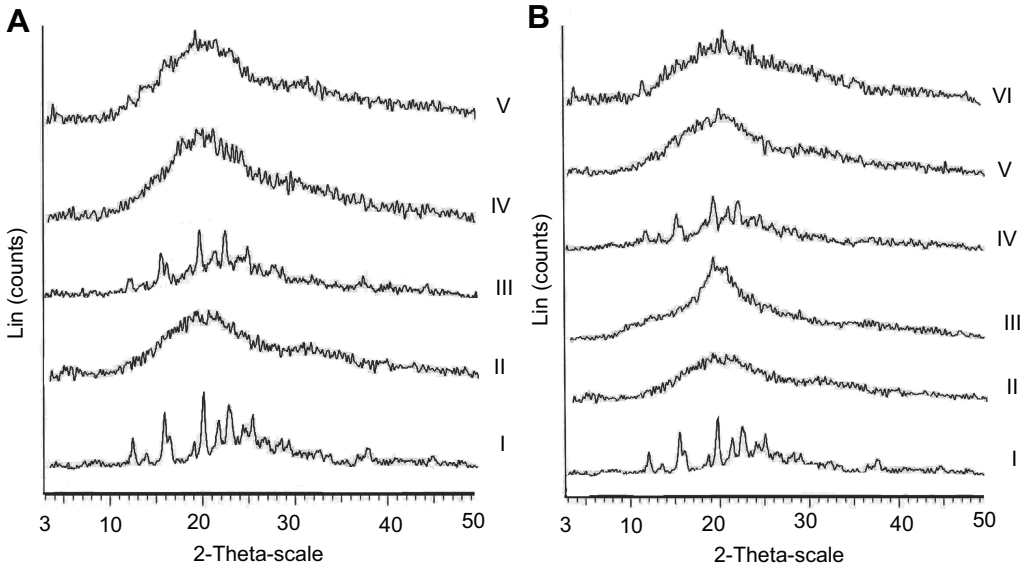

Figure 5 X-ray diffractometry.
Notes: (**A**) Uncoated diosmin-PLGA nanoparticles (F5). (I) Diosmin, (II) PLGA, (III) diosmin:PLGA 1:1 PM, (IV) plain uncoated nanoparticles, and (V) medicated uncoated PLGA nanoparticles. (**B**) Chitosan-coated PLGA nanoparticles (F14). (I) Diosmin, (II) PLGA, (III) chitosan, (IV) diosmin:chitosan 1:1 PM, (V) plain chitosan-coated nanoparticles, and (VI) medicated chitosan-coated nanoparticles.
Abbreviations: PLGA, poly (d,l-lactide-co-glycolide); PM, physical mixture.

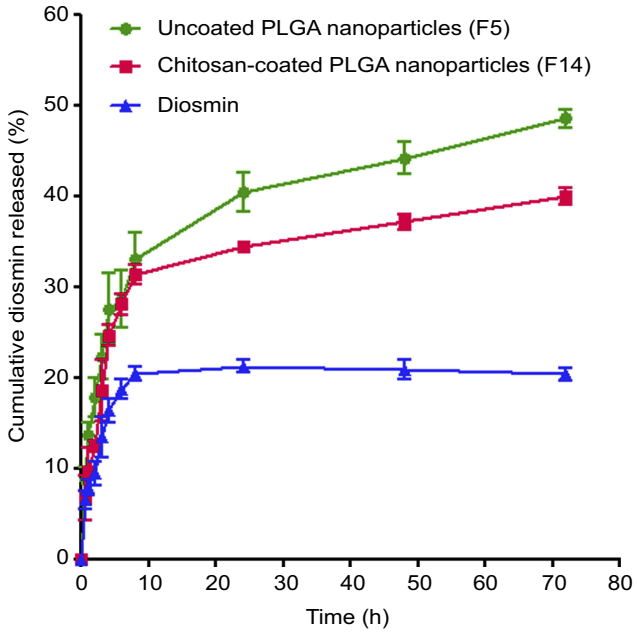

Figure 6 In vitro diosmin release in borate buffer (pH 10.5) from the selected nanoparticles compared to the drug alone.
Abbreviation: PLGA, poly(d,l-lactide-co-glycolide).

Apremilast from PLGA nanoparticles.[53] Non-Fickian mechanism (n<0.45) was found to describe the drug release during the rapid release phase from both types of nanoparticles indicating that both diffusion and erosion controlled the drug release during this phase. Fickian diffusion could be suggested to control the drug release during the sustained release phase since 0.45>n>0.87.[33]

Stability study

Tables 4 and 5 represent the results of the stability study at refrigerator and room temperatures over a period of 3 months, respectively. At refrigerator temperature, there was an insignificant change in average EE%, drug retention%, and ζ-potential of both types of nanoparticles over the 3 months when compared to those initially determined at the beginning of the storage period. Similar results were observed at room temperature except that a significant (P<0.05) decrease in EE% and drug retention% of the uncoated nanoparticles was recorded at the third month. Uniform size distribution of both types of nanoparticles was indicated by mean PDI values of ≤0.52±0.01 over the storage period at both temperatures. Compared to the initially determined mean particles size, there was a significant increase (P<0.05) in average size of uncoated nanoparticles only at both temperatures over the 3 months; yet, the average particles diameter was ≤233.20±4.50 nm. The higher ζ-potential recorded for coated nanoparticles may explain their higher stability against size enlargement on storage for 3 months at both temperatures. These results collectively can suggest further investigation of both uncoated and coated nanoparticles (F5 and F14, respectively) regarding mucoadhesion and AA.

Mucoadhesion study

Figure 7 shows SEM microphotographs of stomach and duodenum of the different groups orally treated with the selected uncoated (F5) or coated (F14) nanoparticles in comparison with the free drug suspension in 1% w/v CMC. SEM images of stomach and duodenum were recorded at 2 and 8 h post oral treatment (Figure 7A and B, respectively).

After 2 or 8 h, no free diosmin could be detected in stomach (I) or duodenum (II). Uncoated PLGA nanoparticles appeared in both stomach (III) and duodenum (IV) at 2-h post-dosing, while their presence after 8 h could be detected only in duodenum (IV). These results may be attributed to the lack of the bioadhesive capability of PLGA, hence the uncoated nanoparticles did not exhibit gastric retention and

Table 3 Kinetic analysis of drug release data

Formula code	Correlation coefficient (r^2)			Release order	Korsmeyer		Main transport mechanism
	Zero order	First order	Higuchi model		n	r^2	
Uncoated PLGA nanoparticles (F5)							
Rapid release phase	0.887	0.889	0.937	Higuchi	0.485	0.957	Non-Fickian
Sustained release phase	0.865	0. 885	0.904	Higuchi	0.170	0.901	Fickian
Coated nanoparticles (F14)							
Rapid release phase	0.915	0.922	0.942	Higuchi	0.599	0.902	Non-Fickian
Sustained release phase	0.939	0.943	0.950	Higuchi	0.107	0.930	Fickian

Abbreviations: PLGA, poly (d,l-lactide-co-glycolide); n, diffusional exponent.

Table 4 Storage stability of the lyophilized selected uncoated and coated nanoparticles at refrigerator temperature (4±1°C)

Month	Size (nm)	PDI	EE%	Drug retention (%)	ζ-potential (mV)
Uncoated nanoparticles (F5)					
0	140.30±1.50	0.20±0.15	75.30±2.60	–	−10.50±0.20
1	155.90±3.10**	0.30±0.05	73.50±7.30	97.39±6.20	−11.70±0.30
2	197.80±4.40***	0.26±0.13	68.00±2.80	95.40±2.90	−9.70±0.49
3	233.20±4.50***	0.40±0.030	71.90±4.70	90.20±0.58	−10.70±0.30
Coated nanoparticles (F14)					
0	337.60±41.00	0.30±0.09	67.40±2.90	–	27.40±2.90
1	345.40±15.90	0.30±0.10	64.60±2.10	95.70±1.10	29.40±1.70
2	378.50±6.60	0.49±0.01	65.30±5.10	96.70±3.50	29.40±1.00
3	379.60±20.90	0.49±0.01	65.20±4.70	96.50±3.30	24.60±0.80

Notes: Data are expressed as mean±SD (n=3). **$P<0.01$ and ***$P<0.001$ vs initially determined size at the beginning of the storage period.
Abbreviations: PDI, polydispersity index; EE%, entrapment efficiency percentage.

Table 5 Storage stability of the lyophilized selected uncoated and coated nanoparticles at room temperature (25±1°C)

Month	Size (nm)	PDI	EE%	Drug retention (%)	ζ-potential (mV)
Uncoated nanoparticles (F5)					
0	155.9±3.1	0.2±0.15	75.3±2.6	–	−10.5±0.2
1	175.5±6.3*	0.4±0.02	72.4±5.5	96.25±8.5	−10.9±0.9
2	192.2±8.6***	0.48±0.006	69.2±4.7	91.75±3	−10.6±0.8
3	230.9±1***	0.42±0.08	60.6±6.1*	80.3±5.6*	−10.6±0.4
Coated nanoparticles (F14)					
0	337.6±41	0.3±0.09	67.4±2.9	–	27.4±2.9
1	386.7±15.9	0.5±0.03	64.2±3	95.2±0.4	26.6±1.3
2	367.8±12.4	0.47±0.08	65±4.6	96.3±3.1	23.3±1.1
3	385.7±10.1	0.52±0.01	64.4±4.6	95.4±1.1	21.4±1.3

Notes: Data are expressed as mean±SD (n=3). *$P<0.05$ vs initially determined size at the beginning of the storage period or drug retention % at the first month, ***$P<0.001$ vs initially determined size at the beginning of the storage period.
Abbreviations: PDI, polydispersity index; EE%, entrapment efficiency percent.

passed down to duodenum. In contrast, chitosan-coated nanoparticles were observed in stomach (V) in a massive amount even at 8-h post-dosing, while minor amount were noticed in the duodenum (VI). This confirms the high gastric retention potential of chitosan-coated nanoparticles (F14). As revealed by ζ-potential measurements, chitosan imparted positive charge on the coated nanoparticles, and hence mucoadhesion can be promoted through their electrical interaction with the negatively charged mucus.[54]

In vivo evaluation

Macroscopic examination

Figure 8 represents gross appearance of freshly excised gastric tissue of different groups orally pretreated with either free drug suspension in 1% w/v CMC or the selected nanoparticles. Parameters describing the AA through macroscopic examination are illustrated in Table 6. Apparently normal gastric mucosa was seen in normal control (group I) (Figure 8A). On the other hand, glandular mucosal ulcerations as well as glandular and non-glandular mucosal congestion and edema were extensive in gastric tissues of rats of positive control group (II) (Figure 8B). Accordingly, an incidence of ulcer equal to 100% and the highest Paul's index of 25 were observed in case of positive control rats. Oral pretreatment with free diosmin (100 mg/kg) resulted in moderate glandular mucosal ulcerations, glandular and non-glandular mucosal congestion and edema (Figure 8C). Mild congestion and edema appeared in glandular and non-glandular gastric mucosa in group IV rats that orally received uncoated nanoparticles (Figure 8D). Apparently normal gastric mucosa was seen in rats pretreated with coated nanoparticles (Figure 8E). In agreement, the three

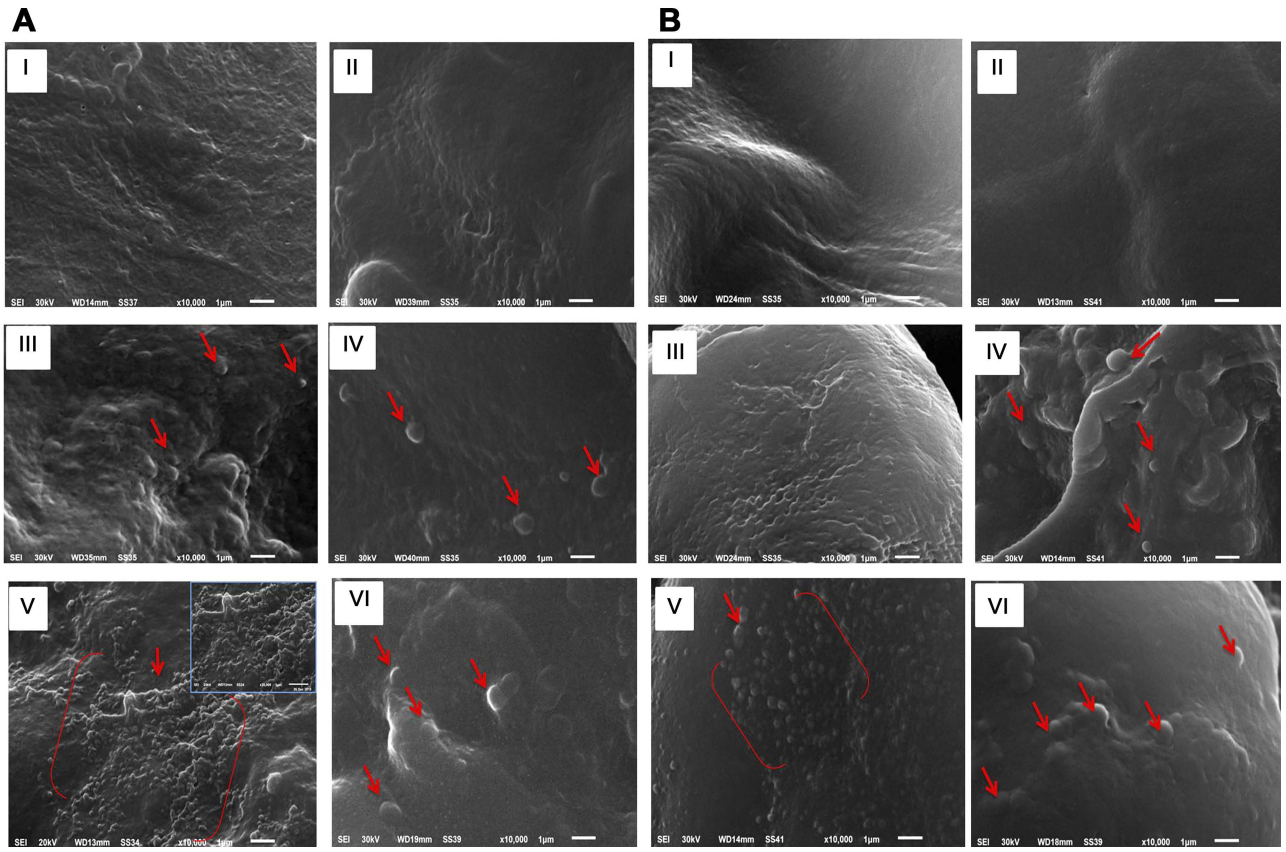

Figure 7 Scanning electron microscopy of stomach and duodenum of the different groups orally treated with diosmin (100 mg/kg) or an equivalent dose of either uncoated or chitosan-coated nanoparticles.
Notes: (**A**) Two-hour post-dosing and (**B**) eight-hour post-dosing. (I) and (II) stomach and duodenum of rats treated with diosmin, respectively, (III) and (IV) stomach and duodenum of rats that administered uncoated PLGA nanoparticles, respectively, (V) and (VI) stomach and duodenum of rats given chitosan-coated nanoparticles, respectively. Arrows point to the attached nanoparticles.
Abbreviation: PLGA, poly(d,l-lactide-co-glycolide).

pretreatment groups (III, IV, and V) showed significantly ($P<0.05$) lower mean ulcers number when compared to positive control rats (II). Hence, highly diminished ulcer incidence and Paul's index values were estimated for these groups relative to positive control. In comparison with rats orally pretreated with free diosmin, a greater AA was obtained on oral pretreatment with uncoated PLGA nanoparticles. Coating of PLGA nanoparticles with chitosan resulted in highly potentiated AA of diosmin.

More prolonged residence time of nanoparticles in ulcerative tissues can be expected due to the greater accumulation and the facilitated uptake by immune cells, such as macrophages.[55]

The greater AA of the coated nanoparticles than the uncoated ones can be attributed to the adherence of the positively charged chitosan-coated nanoparticles to the negatively charged cellular membranes[56] as well as their escape from the acidic solution of endosomes–lysosomes,[57] thus inducing their intracellular uptake into the cytoplasm. The interaction with the cellular membrane results in a structural reorganization of junction proteins that is reversed when the contact with chitosan is terminated.[58] Moreover, mucoadhesion enhanced through the electrical interaction of positively charged chitosan-coated nanoparticles with the negatively charged mucin can still account for the potentiated AA.[54] In spite of these biological interactions due to the positively charged surface of chitosan-coated nanoparticles, chitosan cytotoxicity was negated as clarified by cell viability close to 100% after contacting with chitosan or systems based on it.[59] In addition, no significant toxicity was reported following repeated oral administration of microparticles or nanoparticles incorporating chitosan at a dose range of 100–125 mg/kg as revealed by the absence of abnormalities in hepatic and renal functions or pathological changes in liver, kidney, and intestinal segments.[60,61]

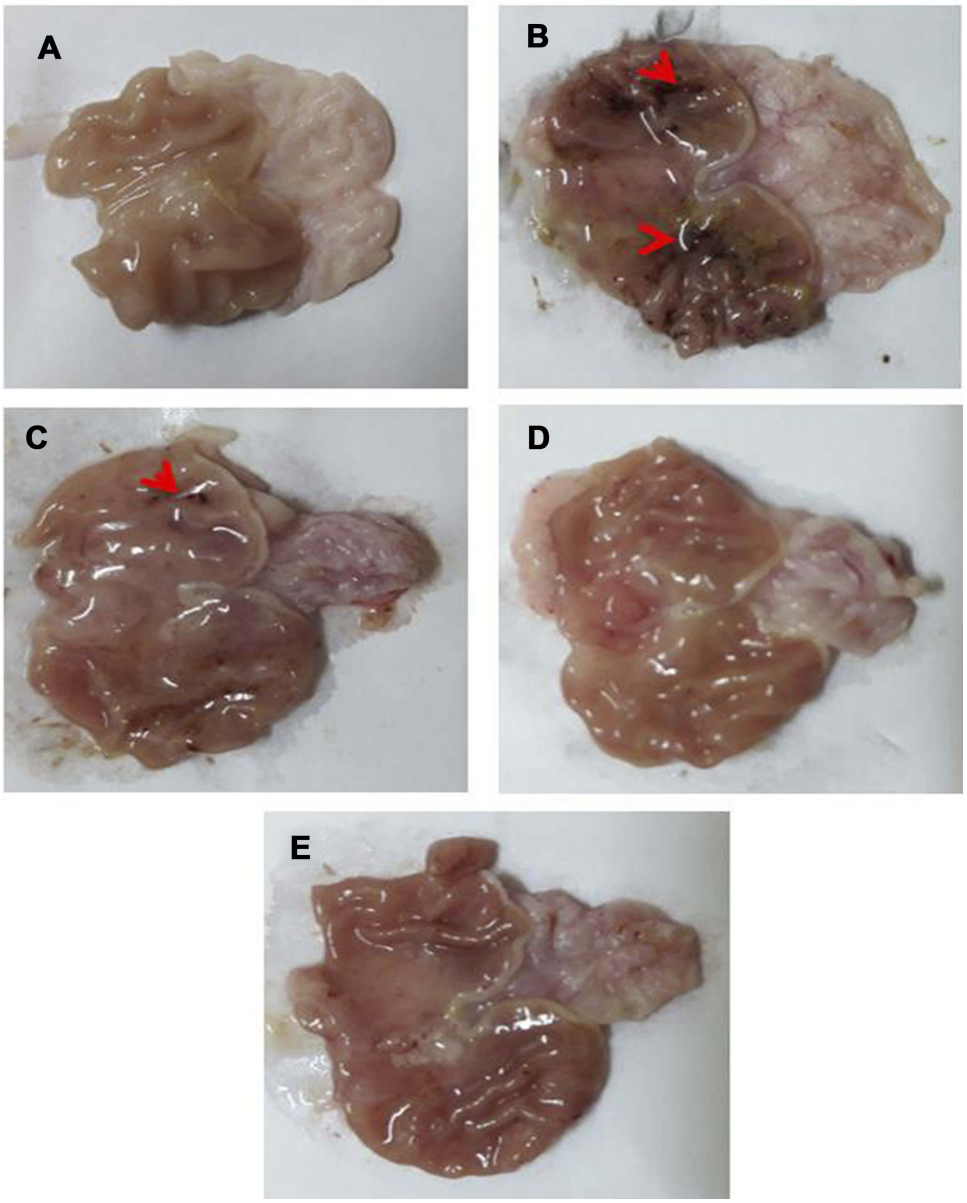

Figure 8 Gross appearance of freshly excised stomachs.
Notes: (**A**) Normal control with normal gastric mucosa. (**B**) Positive control showing glandular mucosal ulcerations (red arrowheads) as well as extensive glandular and non-glandular mucosal congestion and edema. (**C**) Rats pretreated with diosmin (100 mg/kg) displaying moderate glandular mucosal ulcerations (red arrowheads), glandular and non-glandular mucosal congestion and edema were moderate. (**D**) Rats pretreated with an equivalent dose of uncoated PLGA nanoparticles exhibiting mild congestion and edema appeared in glandular and non-glandular gastric mucosa. (**E**) Apparently normal gastric mucosa of rats pretreated with an equivalent dose of chitosan-coated nanoparticles.
Abbreviation: PLGA, poly(d,l-lactide-co-glycolide).

Histopathological examination

Figure 9 displays microphotographs of histopathological examination (HE, 100×) of non-glandular (A) and glandular (B) gastric tissues of the different groups. Normal control (I) displayed an intact architecture of non-glandular and glandular gastric wall (I). Administration of ethanol to rats of positive control (II) triggered a severe gastric injury with high scores of microscopic damage including extensive congestion and edema in non-glandular portion, mucosal ulceration and submucosal inflammation in glandular portion. Submucosal congestion and edema in non-glandular and glandular portions besides submucosal inflammation in glandular portion were moderate in rats pretreated with free diosmin (III), while mild in rats that administered uncoated nanoparticles (IV). Non-glandular and glandular gastric walls retained their normal histological pictures in rats that received chitosan-coated nanoparticles (V).

Table 6 Parameters of macroscopical evaluation of ethanol-induced ulcers in rats

Animal group	Number of ulcers	Percentage incidence of animals	Paul's index	AA	Severity of inflammation
	Mean±SD n=6				
I (normal control)	–	0	0	–	– (no inflammation)
II (positive control)	25±5.67	100	25	–	+++ (severe)
III (diosmin)	9±3.37*	66.67	6	4.16	++ (moderate)
IV (uncoated PLGA nanoparticles)	4±2***	50	2	12.5	+ (mild)
V (chitosan-coated nanoparticles)	2±1.26***	33.33	0.667	37.48	+ (mild)

Notes: 100 mg/kg diosmin or an equivalent dose of the nanoparticles was used; *$P<0.05$ and ***$P<0.001$ vs positive control group (II).
Abbreviations: PLGA, poly(lactic-co-glycolic) acid; AA, anti-ulcer activity.

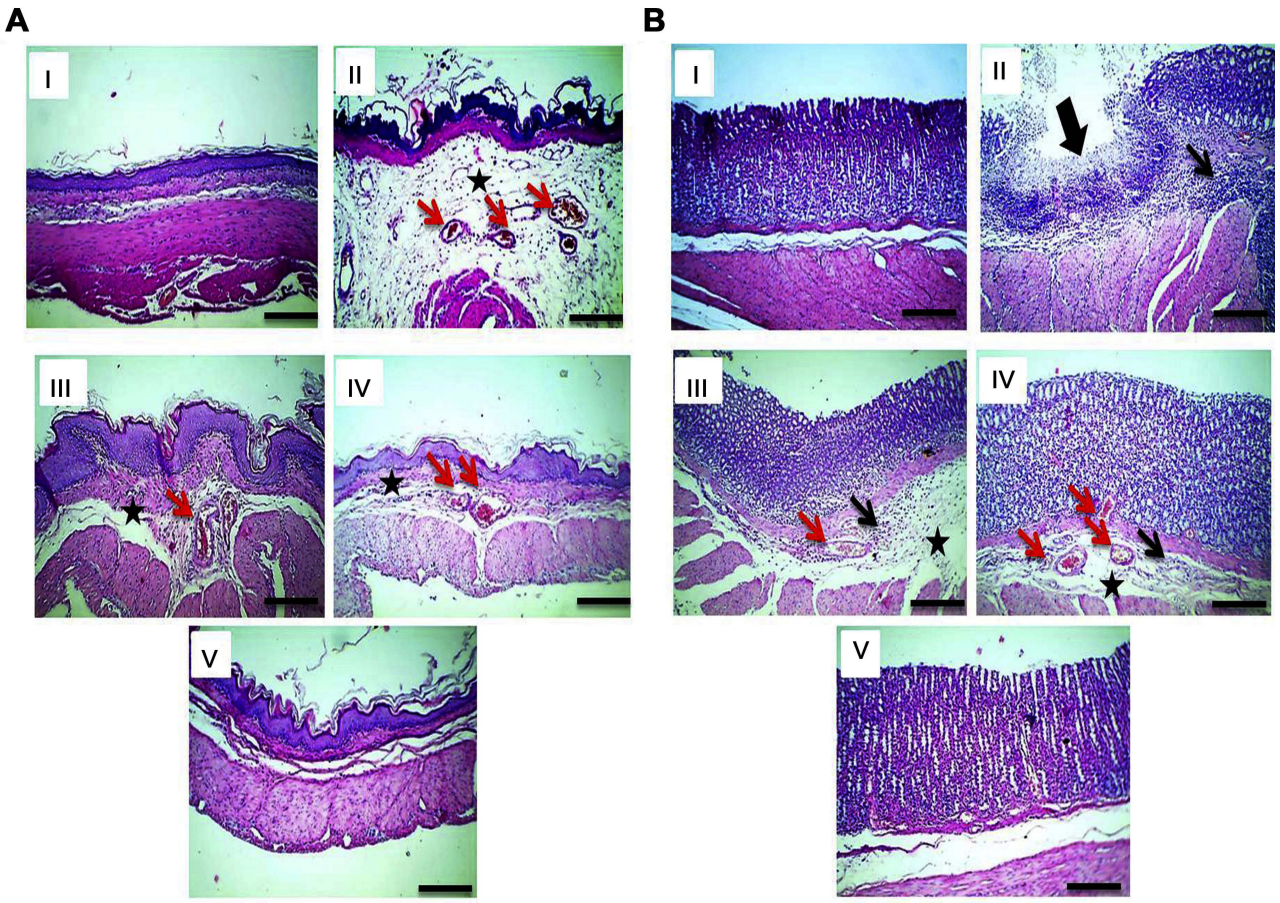

Figure 9 Histological examination (HE, 100x) of gastric tissues.
Notes: (**A**) Non-glandular and (**B**) glandular gastric mucosa. (I) Normal control displaying an intact architecture of non-glandular and glandular gastric wall. (II) Positive control showing extensive congestion (red arrows) and edema (black asterisk) in non-glandular portion, mucosal ulceration (thick black arrow), and submucosal inflammation (thin black arrow) in glandular portion. (III)Rrats pretreated with diosmin (100 mg/kg) displaying moderate submucosal congestion (red arrows) and edema (black asterisk) in non-glandular and glandular portions besides submucosal inflammation (thin black arrow) in glandular portion. (IV) Rats pretreated with uncoated PLGA nanoparticles exhibiting mild submucosal congestion (red arrows) and edema (black asterisk) in non-glandular and glandular portions besides very mild submucosal inflammatory cells infiltration in glandular portion (thin black arrow). (V) Non-glandular and glandular gastric walls retained their normal histological pictures in rats pretreated with chitosan-coated nanoparticles.
Abbreviation: PLGA, poly(d,l-lactide-co-glycolide).

In general, oral pretreatment with diosmin either free or as nanoparticles lowered the pathologic scores and attenuated the gastric damage. Results of statistical analysis of histopathological examination in glandular portion of gastric tissues are depicted in Figure 10A–D. The results revealed that there was a significant

(P<0.05) elevation in epithelial cells loss, edema, congestion, and inflammation in glandular portions of positive control and rats orally pretreated with free diosmin or uncoated nanoparticles when compared to normal control. In contrast to free diosmin, oral pretreatment with either uncoated or coated nanoparticles significantly (P<0.05) lowered epithelial cells loss, edema, congestion, and inflammation in glandular portions relative to positive control. In comparison with free diosmin, there was a significant (P<0.05) reduction in these pathological changes only following oral administration of coated nanoparticles.

Significantly (P<0.05) elevated edema in non-glandular portions of gastric tissues was observed in positive control and rats orally pretreated with either free diosmin or uncoated nanoparticles than normal rats (Figure 10E). Rats administered coated nanoparticles encountered a significantly (P<0.05) lower edema in non-glandular portions than positive control, free diosmin, and uncoated nanoparticles. Regarding congestion in non-glandular gastric tissues, there was a significant (P<0.05) increase in positive control and rats pretreated with free diosmin relative to normal control (Figure 10F). Significantly (P<0.05) diminished congestion was obtained in the three pretreatment

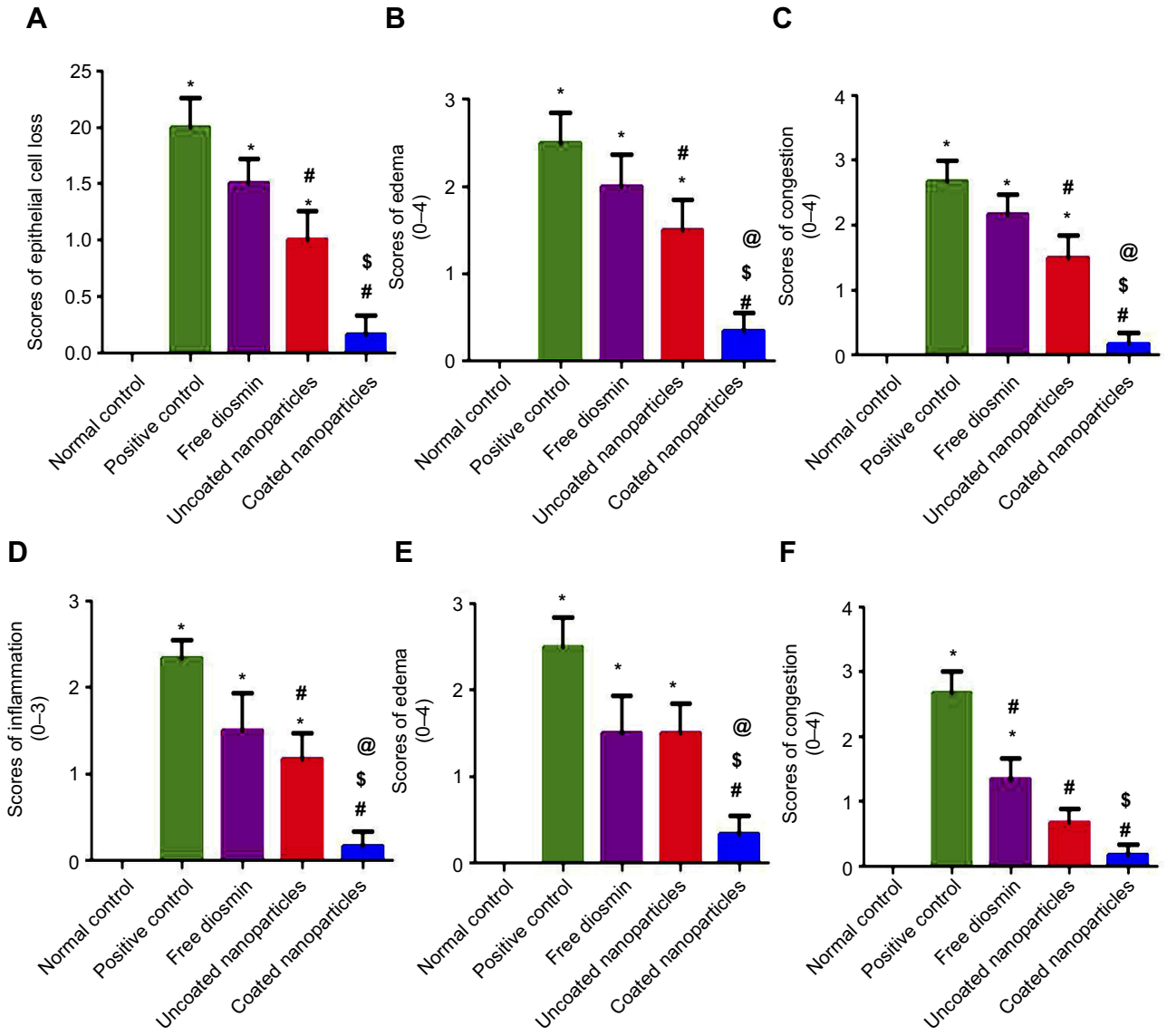

Figure 10 Statistical analysis of microscopic histopathological scores in gastric mucosa.
Notes: (**A**–**D**) Glandular and (**E** and **F**) non-glandular mucosa. Data are mean±SD, n=6; statistical differences at P<0.05 considered significant; *vs normal control group; #vs positive control group; $vs diosmin (100 mg/kg) pretreated group; @vs group pretreated with an equivalent dose of uncoated PLGA nanoparticles.
Abbreviation: PLGA, poly(d,l-lactide-co-glycolide).

groups when compared to positive control. In contrast to uncoated nanoparticles, oral administration of coated nanoparticles resulted in a significantly (P<0.05) lower congestion in non-glandular gastric tissue than rats given free diosmin. There was insignificant difference between rats orally pretreated with uncoated and coated nanoparticles regarding congestion scores in non-glandular portion.

There was insignificant difference between normal control and rats received coated nanoparticles regarding severity of all pathological changes describing ulceration in both glandular and non-glandular gastric tissues. Thus, it can be said that coating of PLGA nanoparticles with chitosan significantly potentiated the cytoprotective activity of diosmin against ethanol-induced ulcer in rats. These results may be due to the increased interaction with the negatively charged cellular membranes and the improved intracellular uptake into the cytoplasm,[56] as well as the enhanced escape from the acidic solution of endosomes–lysosomes into the cytoplasm.[57] Moreover, the increased mucoadhesion of positively charged chitosan-coated nanoparticles with the negatively charged mucin and the resulting gastric retention (Figure 7) can still explain the superiority of coated nanoparticles.[54]

Immunohistochemical loclization of NF-κB

Figure 11 illustrates immunohistochemical evaluation of NF-κB expression in non-glandular (A) and glandular (B) gastric tissues. Mild positive expression was recognized in both tissues in normal control group (I). Strong immunoreactivity was observed in both mucosae particularly around area of mucosal damage and stained inflammatory cells infiltrating submucosa of glandular portion in positive control (II). Oral pretreatment with free diosmin suspension in 1%w/v CMC (100 mg/kg, III) or an equivalent

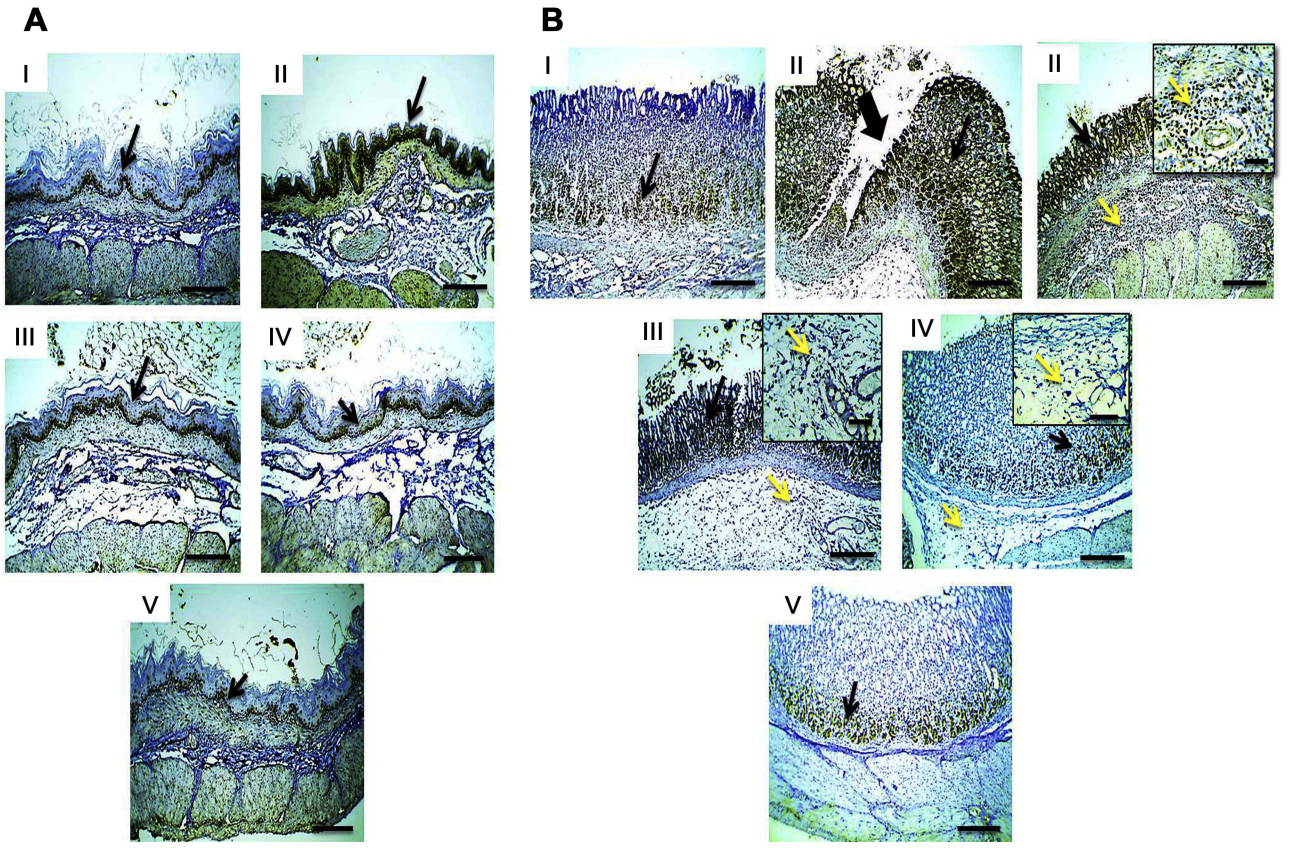

Figure 11 Microscopic pictures of rats stomach immunostained against NF-κB.
Notes: (**A**) Non-glandular and (**B**) glandular gastric mucosa. (I) Normal control showing mild positive expression in glandular and non-glandular gastric mucosa. (II) Positive control rats displaying strong positive expression in glandular and non-glandular gastric mucosa particularly around area of mucosal damage (thick black arrow) and stained inflammatory cells infiltrating submucosa of glandular portion. (III) Rats pretreated with diosmin (100 mg/kg) or (IV) an equivalent dose of uncoated PLGA nanoparticles exhibiting mild positive expression in non-glandular mucosa, as well as moderate positive expression in gastric mucosa and the inflammatory cells infiltrating submucosa of glandular portion. (V) Rats that received chitosan-coated nanoparticles showing mild positive expression in glandular and non-glandular gastric mucosa. Thin black arrows point to positive signal in mucosa and thin yellow arrows point to positively stained leukocytes infiltrating submucosa. IHC counterstained with Mayer's hematoxylin (100×), insert (S, 200×).
Abbreviations: NF-κB, nuclear factor kappa-light-chain-enhancer of activated B cells; PLGA, poly (d,l-lactide-co-glycolide); IHC, immunohistochemistry.

dose of uncoated nanoparticles (IV) resulted in mild immunostaining in non-glandular mucosa, meanwhile, moderate positive expression and the inflammatory cells infiltrating submucosa of glandular portion were recorded in gastric mucosa (III and IV, respectively). Mild positive expression was detected in both mucosae in rats that received chitosan-coated nanoparticles (V).

Results of statistical analysis of immunohistochemical localization of gastric NF-κB in glandular (A) and non-glandular portions (B) are depicted in Figure 12. According to this figure, there was a significant (P<0.05) increase in gastric NF-κB expression in both portions in positive control when compared to normal control. Oral pretreatment with free diosmin suspension insignificantly affect the immunoreactivity. On the other hand, there was a significant (P<0.05) reduction in glandular and non-glandular NF-κB expression following oral administration of diosmin loaded nanoparticles either coated or uncoated in comparison with the positive control. In agreement with histopathological examination, the superiority of coated nanoparticles over the uncoated ones can be suggested by the significantly (P<0.05) lower glandular and non-glandular NF-κB expression than that produced by either free diosmin or uncoated nanoparticles as well as the insignificantly different glandular and non-glandular NF-κB expression from that recorded in normal group. Such superiority can still be attributed to the increased intracellular uptake into the cytoplasm[57] as well as the improved mucoadhesion and gastric retention of these positively charged nanoparticles.[54]

TEM examination of the gastric mucosa ultrastructure

TEM examination of the mucosal surface of normal control rats revealed well-arranged microvilli in neat rows with no loss, normal nucleus, high density of mitochondria, regular pattern of rough endoplasmic reticulum, and dispersed gastric secretion (Figure 13A). Meanwhile, the mucosal surface of positive control rats showed swollen mitochondria, deleted rough endoplasmic reticulum, abnormal nucleus, cytoplasmic vacuoles, cells with dilated reticulum, complete loss of microvilli, and several non-homogenated cytoplasmic inclusions (Figure 13B). Following oral treatment with free diosmin suspension, there was a slight amelioration in the mucosal cells, yet wide junctions between cells were observed and some cytoplasmic organelles were still deleterious, including swollen mitochondria, pyknotic nucleus, and irregular microvilli (Figure 13C). Regarding rats that received uncoated PLGA nanoparticles, a slightly ameliorated

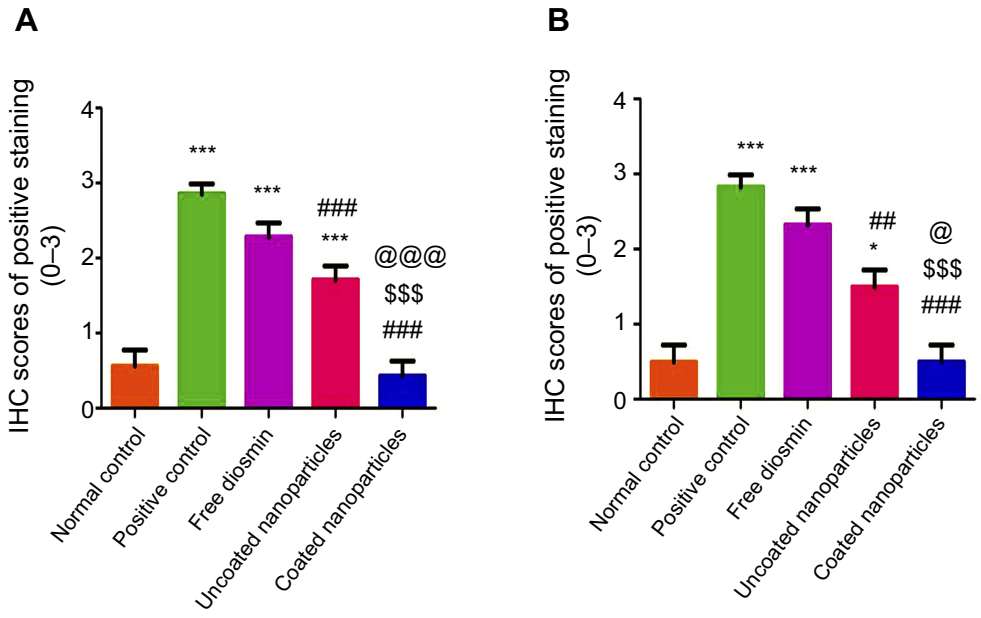

Figure 12 Statistical analysis of IHC scores of NF-κB in gastric mucosa.
Notes: (**A**) Glandular and (**B**) non-glandular mucosa. Data are mean±SD, n=6;
*P<0.05 and ***P<0.001 vs normal control; ###P<0.01 and ####P<0.001 vs positive control; $$$$P$<0.001 vs diosmin (100 mg/kg) pretreated group; @P<0.05 and @@@P<0.001 vs group pretreated with an equivalent dose of uncoated PLGA nanoparticles.
Abbreviations: IHC, immunohistochemistry; NF-κB, nuclear factor kappa-light-chain-enhancer of activated B cells; PLGA, poly(d,l-lactide-co-glycolide).

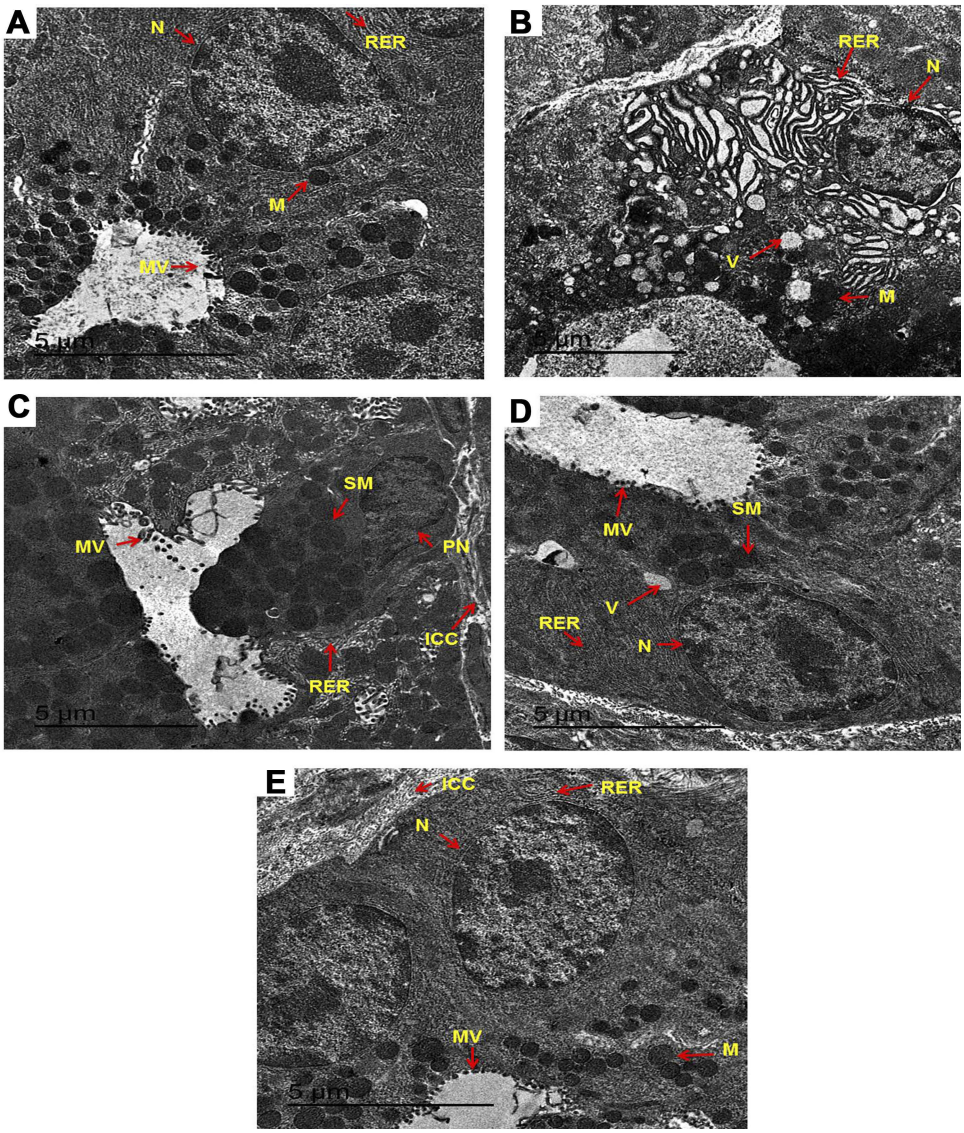

Figure 13 TEM examination of the gastric mucosa ultrastructure.
Notes: (**A**) Normal control rats showing well-arranged microvilli in neat rows with no loss, normal nucleus, high density of mitochondria, regular pattern of rough endoplasmic reticulum, and dispersed gastric secretion. (**B**) Positive control rats displaying swollen mitochondria, deleted rough endoplasmic reticulum, abnormal nucleus, cytoplasmic vacuoles, cells with dilated reticulum, complete loss of microvilli, and several non-homogenated cytoplasmic inclusions. (**C**) Rats pretreated with free diosmin (100 mg/kg) exhibited a slight amelioration in the mucosal cells, wide junctions between cells and some deleterious cytoplasmic organelles including swollen mitochondria, pyknotic nucleus, and irregular microvilli. (**D**) Rats that received uncoated PLGA nanoparticles showing a slightly ameliorated mitochondria, normal rough endoplasmic reticulum, intact cell membrane, and regular microvilli. (**E**) Rats pretreated with chitosan-coated nanoparticles of diosmin showing obvious amelioration in the mucosal cells, disappearance of vacuoles, intact cell membrane with tight junctions and regularly arranged microvilli with high density as well as normal mitochondria, endoplasmic reticulum, and nucleus.
Abbreviation: TEM, transmission electron microscopy.

mitochondria, normal rough endoplasmic reticulum, intact cell membrane, and regular microvilli were observed in the mucosal surface (Figure 13D). Oral pretreatment with chitosan-coated nanoparticles of diosmin resulted in obvious amelioration in the mucosal cells, disappearance of vacuoles, intact cell membrane with tight junctions and regularly arranged microvilli with high density as well as normal mitochondria, endoplasmic reticulum, and nucleus (Figure 13E).

Conclusion

The selected uncoated nanoparticles consisted of 1:15 drug-PLGA weight ratio using 20 mg diosmin and methylene chloride as an organic phase because they showed the highest EE% (75.30±2.60%) and particle size <200 nm (155.90±3.10 nm). Coating of these nanoparticles with chitosan (0.10%, 0.15%, and 0.30% w/v) significantly enlarged the size on the increase of chitosan concentration but EE% did not significantly differ; thus, those coated

with 0.10% w/v were further investigated in comparison with the selected uncoated PLGA nanoparticles. The nanoscopic size and spherical shape were confirmed using SEM and TEM. FT-IR, DSC, and XRD results clarified the absence of drug peaks in the recorded data of the medicated nanoparticles suggesting drug encapsulation within them. The selected uncoated nanoparticles possessed lower potential (−10.50±0.20 mV) than those coated with 0.10% w/v chitosan (+27.40±2.90 mV). This may explain the higher stability of coated nanoparticles against size enlargement on storage for 3 months. The optimized coated nanoparticles exhibited gastric retention as indicated by SEM examination. As well, these nanoparticles caused a significant decrease in mucosal damage, the majority of histopathological alterations and NF-κB expression in glandular and non-glandular portions of gastric tissue when compared to positive control, free diosmin and uncoated nanoparticles. The superiority of coated nanoparticles was revealed by the insignificant difference of the macroscopical damage, histopathological alterations, and NF-κB expression relative to normal control as well as the preservation of normal ultrastructure of the gastric mucosa as revealed by TEM. Therefore, the optimized chitosan-coated nanoparticles can be suggested as a promising oral drug delivery system of diosmin.

Acknowledgment

The authors would like to thank Dr Walaa Awadin, Associate Professor, Department of Pathology, Faculty of Veterinary Medicine, Mansoura University, for her technical support and specimens examination during macroscopical and histopathological evaluation as well as immunohistochemical localization of NF-κB. The authors would also like to thank Dr Abd El-Fattah BM El-Beltagy, Associate Professor, Department of Zoology, Faculty of Science, Damanhour University, for examination of the ultrastructure of the gastric mucosa by TEM. The authors are grateful for Purac Biomaterials, Holland for kindly supplying the poly(lactic-co-glycolic acid (PLGA).

Disclosure

The authors report no conflicts of interest in this work.

References

1. Konturek SJ, Konturek PC, Pawlik T, Sliwowski Z, Ochmański W, Hahn EG. Duodenal mucosal protection by bicarbonate secretion and its mechanisms. *J Physiol Pharmacol*. 2004;55(2):5–17.
2. Bruntan LL, Lazo JS, Parker KL. *Goodman and Gilman's: The Pharmacological Basis of Therapeutics*. 11th ed. New York: McGraw Hill Companies; 2006.
3. Ai F, Ma Y, Wang J, Li Y. Preparation, physicochemical characterization and in-vitro dissolution studies of diosmin-cyclodextrin inclusion complexes. *Iran J Pharm Res*. 2014;13(4):1115–1123.
4. Tong N, Zhang Z, Zhang W, et al. Diosmin alleviates retinal edema by protecting the blood-retinal barrier and reducing retinal vascular permeability during ischemia/reperfusion injury. *PLoS One*. 2013;8(4):e61794. doi:10.1371/journal.pone.0061794
5. Vrbata P, Berka P, Stránská D, Doležal P, Lázníček M. Electrospinning of diosmin from aqueous solutions for improved dissolution and oral absorption. *Int J Pharm*. 2014;473(1–2):407–413. doi:10.1016/j.ijpharm.2014.07.017
6. Anwer MK, Jamil S, Ansari MJ, et al. Water soluble binary and ternary complexes of diosmin with β-cyclodextrin: spectroscopic characterization, release studies and anti-oxidant activity. *J Mol Liq*. 2014;199:35–41. doi:10.1016/j.molliq.2014.08.012
7. Arab HH, Salama SA, Omar HA, Arafa E-SA, Maghrabi IA. Diosmin protects against ethanol-induced gastric injury in rats: novel anti-ulcer actions. *PLoS One*. 2015;10(3):e0122417. doi:10.1371/journal.pone.0122417
8. Russo R, Chandradhra D, De Tommasi N. Comparative bioavailability of two diosmin formulations after oral administration to healthy volunteers. *Molecules*. 2018;23(9):pii:E2174. doi:10.3390/molecules23092174
9. Freag MS, Elnaggar YS, Abdallah OY. Development of novel polymer-stabilized diosmin nanosuspensions: in vitro appraisal and ex vivo permeation. *Int J Pharm*. 2013;454(1):462–471. doi:10.1016/j.ijpharm.2013.06.039
10. Kawashima Y, Yamamoto H, Takeuchi H, Kuno Y. Mucoadhesive DL- lactide/glycolide copolymer nanospheres coated with chitosan to improve oral delivery of elcatonin. *Pharm Dev Technol*. 2000;5(1):77–85. doi:10.1081/PDT-100100522
11. Garner RC, Garner JV, Gregory S, Whattam M, Calam A, Leong D. Comparison of the absorption of micronized (Daflon 500 mg) and non-micronized 14C-diosmin tablets after oral administration to healthy volunteers by accelerator mass spectrometry and liquid scintillation counting. *J Pharm Sci*. 2002;91(1):32–40. doi:10.1002/jps.10052
12. Makadia HK, Siegel SJ. Poly lactic-co-glycolic acid (PLGA) as biodegradable controlled drug delivery carrier. *Polymers (Basel)*. 2011;3(3):1377–1397. doi:10.3390/polym3031377
13. Derman S. Caffeic acid phenethyl ester loaded PLGA nanoparticles: effect of various process parameters on reaction yield, encapsulation efficiency and particle size. *J Nanomater*. 2015;16:1–12. doi:10.1155/2015/341848
14. Sanna V, Roggio AM, Siliani S, et al. Development of novel cationic chitosan- and anionic alginate–coated poly(d,l-lactide-co-glycolide) nanoparticles for controlled release and light protection of resveratrol. *Int J Nanomedicine*. 2012;7:5501–5516. doi:10.2147/IJN.S36684
15. Kim BS, Kim CS, Lee KM. The intracellular uptake ability of chitosan-coated poly (d,l-lactideco-glycolide) nanoparticles. *Arch Pharm Res*. 2008;31(8):1050–1054. doi:10.1007/s12272-001-1267-5
16. Nafee N, Taetz S, Schneider M, Schaefer UF, Lehr CM. Chitosan-coated PLGA nanoparticles for DNA/RNA delivery: effect of the formulation parameters on complexation and transfection of antisense oligonucleotides. *Nanomedicine*. 2007;3(3):173–183. doi:10.1016/j.nano.2007.03.006
17. Slütter B, Bal S, Keijzer C, et al. Nasal vaccination with N-trimethyl chitosan and PLGA based nanoparticles: nanoparticle characteristics determine quality and strength of the antibody response in mice against the encapsulated antigen. *Vaccine*. 2010;28(38):6282–6291. doi:10.1016/j.vaccine.2010.06.121

18. Zhang X, Sun M, Zheng A, Cao D, Bi Y, Sun J. Preparation and characterization of insulin loaded bioadhesive PLGA nanoparticles for oral administration. *Eur J Pharm Sci*. 2012;45(5):632–638. doi:10.1016/j.ejps.2012.01.002
19. Wang Y, Li P, Kong L. Chitosan modified PLGA nanoparticles with versatile surface for improved drug delivery. *AAPS PharmSciTech*. 2013;14(2):585–592. doi:10.1208/s12249-013-9943-3
20. Alqahtani S, Simon L, Astete CE, et al. Cellular uptake, antioxidant and antiproliferative activity of entrapped α-tocopherol and γ-tocotrienol in poly(lactic-co-glycolic) acid (PLGA) and chitosan covered PLGA nanoparticles(PLGA-Chi). *J Colloid Interface Sci*. 2015;445:243–251. doi:10.1016/j.jcis.2014.12.083
21. Chronopoulou L, Massimi M, Giardi MF, et al. Chitosan coated PLGA nanoparticles: a sustained drug release strategy for cell cultures. *Colloids Surf B Biointerfaces*. 2013;103:310–317. doi:10.1016/j.colsurfb.2012.10.063
22. Chuah LH, Billa N, Roberts CJ, Burley JC, Manickam S. Curcumin-containing chitosan nanoparticles as a potential mucoadhesive delivery system to the colon. *Pharm Dev Technol*. 2013;18(3):591–599. doi:10.3109/10837450.2011.640688
23. Bigucci F, Luppi B, Cerchiara T, et al. Chitosan/pectin polyelectrolyte complexes: selection of suitable preparative conditions for colon-specific delivery of vancomycin. *Eur J Pharm Sci*. 2008;35(5):435–441. doi:10.1016/j.ejps.2008.09.004
24. Kumar R, Philip A. Gastroretentive dosage forms for prolonging gastric residence time. *Int J Pharm Med*. 2007;21(2):157–171. doi:10.2165/00124363-200721020-00005
25. Mohammadi-Samani S, Taghipour B. PLGA micro and nanoparticles in delivery of peptides and proteins; problems and approaches. *Pharm Dev Technol*. 2015;20(4):385–393. doi:10.3109/10837450.2014.882940
26. Lassalle V, Ferreira ML. PLA nano- and microparticles for drug delivery: an overview of the methods of preparation. *Macromol Biosci*. 2007;7:767–783. doi:10.1002/(ISSN)1616-5195
27. Lai P, Daear W, Löbenberg R, Prenner EJ. Overview of the preparation of organic polymeric nanoparticles for drug delivery based on gelatine, chitosan, poly(d,l-lactide-co-glycolic acid) and polyalkylcyanoacrylate. *Colloids Surf B Biointerfaces*. 2014;118:154–163. doi:10.1016/j.colsurfb.2014.03.017
28. Mahmoodi M, Khosroshahi ME, Atyabi F. Laser thrombolysis and in vitro study of tPA release encapsulated by chitosan coated PLGA nanoparticles for AMI. *Int J Biol Biomed Eng*. 2010;4(2):35–42.
29. Mohamed EA, Abu Hashim II, Yusif RM, et al. Polymeric micelles for potentiated antiulcer and anticancer activities of naringin. *Int J Nanomedicine*. 2018;13:1009–1027. doi:10.2147/IJN.S154325
30. Mittal G, Sahana DK, Bhardwaj V, Ravi Kumar MN. Estradiol loaded PLGA nanoparticles for oral administration: effect of polymer molecular weight and copolymer composition on release behavior in vitro and in vivo. *J Control Release*. 2007;119(1):77–85. doi:10.1016/j.jconrel.2007.02.005
31. Martin AN, Swarbrick J, Cammarata A. *Physical Pharmacy: Physical Chemical Principles in the Pharmaceutical Sciences*. 4th ed. Lea & Febiger, editors. Philadelphia; 1993.
32. Higuchi T. Mechanism of sustained action medication. theoretical analysis of rate of release of solid drugs dispersed in solid matrices. *J Pharm Sci*. 1963;52(12):1145–1149. doi:10.1002/jps.2600521210
33. Ritger PL, Peppas NA. A simple equation for description of solute release I. Fickian and non-Fickian release from non-swellable devices in the form of slabs, spheres, cylinders or discs. *J Control Release*. 1987;5(1):23–36. doi:10.1016/0168-3659(87)90034-4
34. Suwannateep N, Banlunara W, Wanichwecharungruang SP, Chiablaem K, Lirdprapamongkol K, Svasti J. Mucoadhesive curcumin nanospheres: biological activity, adhesion to stomach mucosa and release of curcumin into the circulation. *J Control Release*. 2011;151(2):176–182. doi:10.1016/j.jconrel.2011.01.011
35. El-Maraghy SA, Rizk SM, Shahin NN. Gastroprotective effect of crocin in ethanol-induced gastric injury in rats. *Chem Biol Interact*. 2015;229:26–35. doi:10.1016/j.cbi.2015.01.015
36. Bancroft JD, Stevens A, Turner DR. *Theory and Practice of Histological Techniques*. 4th ed. New York: Churchill Livingstone; 1996.
37. Laine L, Weinstein WM. Histology of alcoholic hemorrhagic "gastritis": a prospective evaluation. *Gastroenterology*. 1988;94(6):1254–1262. doi:10.1016/0016-5085(88)90661-0
38. Budhian A, Siegel SJ, Winey KI. Haloperidol-loaded PLGA nanoparticles: systematic study of particle size and drug content. *Int J Pharm*. 2007;336(2):367–375. doi:10.1016/j.ijpharm.2006.11.061
39. Panyam J, Williams D, Dash A, Leslie-Pelecky D, Labhasetwar V. Solid-state solubility influences encapsulation and release of hydrophobic drugs from PLGA/PLA nanoparticles. *J Pharm Sci*. 2004;93(7):1804–1814. doi:10.1002/jps.20094
40. Mainardes RM, Evangelista RC. Praziquantel-loaded PLGA nanoparticles: preparation and characterization. *J Microencapsul*. 2005b;22(1):13–24. doi:10.1080/02652040400026285
41. Hussein AS, Abdullah N, Fakru'l-Razi A. Optimizing the process parameters for encapsulation of linamarin into PLGAnanoparticles using doublee mulsion solvent evaporation technique. *Adv Polym Tech*. 2013;32(1):E486–E504. doi:10.1002/adv.21295
42. Beck-Broichsitter M, Rytting E, Lebhardt T, Wang X, Kissel T. Preparation of nanoparticles by solvent displacement for drug delivery: a shift in the "ouzo region" upon drug loading. *Eur J Pharm Sci*. 2010;41(2):244–253. doi:10.1016/j.ejps.2010.06.007
43. Song KC, Lee HS, Choung IY, Cho KI, Ahn Y, Choi EJ. The effect of type of organic phase solvents on the particle size of poly(d,l-lactide-co-glycolide) nanoparticles. *Colloids Surf A Physicochem Eng Asp*. 2006;276(1–3):162–167. doi:10.1016/j.colsurfa.2005.10.064
44. Semete B, Booysen LI, Kalombo L, et al. In vivo uptake and acute immune response to orally administered chitosan and PEG coated PLGA nanoparticles. *Toxicol Appl Pharmacol*. 2010;249(2):158–165. doi:10.1016/j.taap.2010.09.002
45. Sahoo KS, Panyama J, Prabhaa S, Labhasetwara V. Residual polyvinyl alcohol associated with poly (D,L-lactide-coglycolide) nanoparticles affects their physical properties and cellular uptake. *J Control Release*. 2002;82(1):105–114. doi:10.1016/S0168-3659(02)00127-X
46. Müller RH, Jacobs C. Buparvaquone mucoadhesive nanosuspension: preparation, optimisation and long-term stability. *Int J Pharm*. 2002;237(1–2):151–161. doi:10.1016/S0378-5173(02)00040-6
47. Yang J, Lee CH, Park J, et al. Antibody conjugated magnetic PLGA nanoparticles for diagnosis and treatment of breast cancer. *J Mater Chem*. 2007;17:2695–2699. doi:10.1039/b702538f
48. Singh G, Kaur T, Kaur R, Kaur A. Recent biomedical applications and patents on biodegradable polymer-PLGA. *Int J Pharmacol Pharm Sci*. 2014;1(2):30–42.
49. Roy P, Das S, Bera T, Mondol S, Mukherjee A. Andrographolide nanoparticles in leishmaniasis: characterization and in vitro evaluations. *Int J Nanomedicine*. 2010;5:1113–1121. doi:10.2147/IJN.S14787
50. Hanafy AS, Farid RM, ElGamal SS. Complexation as an approach to entrap cationic drugs into cationic nanoparticles administered intranasally for Alzheimer's disease management: preparation and detection in rat brain. *Drug Dev Ind Pharm*. 2015;41(12):2055–2068. doi:10.3109/03639045.2015.1062897
51. Salem AE, Mohamed EA, Elghadban HM, Abdelghani GM. Potential combination topical therapy of anal fissure: development, evaluation, and clinical study. *Drug Deliv*. 2018;25(1):1672–1682. doi:10.1080/10717544.2018.1507059
52. Anwer MK, Al-Mansoor MA, Jamil S, Al-Shdefat R, Ansari MN, Shakeel F. Development and evaluation of PLGA polymer based nanoparticles of quercetin. *Int J Biol Macromol*. 2016;92:213–219. doi:10.1016/j.ijbiomac.2016.07.002

53. Anwer MK, Mohammad M, Ezzeldin E, Fatima F, Alalaiwe A, Iqbal M. Preparation of sustained release apremilast-loaded PLGA nanoparticles: in vitro characterization and in vivo pharmacokinetic study in rats. *Int J Nanomedicine*. 2019;14:1587–1595. doi:10.2147/IJN.S195048
54. Barbi Mda S, Carvalho FC, Kiill CP, et al. Preparation and characterization of chitosan nanoparticles for zidovudine nasal delivery. *J Nanosci Nanotechnol*. 2015;15(1):865–874. doi:10.1166/jnn.2015.9180
55. Cortivo R, Vindigni V, Iacobellis L, Abatangelo G, Pinton P, Zavan B. Nanoscale particle therapies for wounds and ulcers. *Nanomedicine*. 2010;5(4):641–656. doi:10.2217/nnm.10.2
56. Prabha S, Zhou W-Z, Panyam J, Labhasetwar V. Size-dependency of nanoparticle-mediated gene transfection: studies with fractionated nanoparticles. *Int J Pharm*. 2002;244(1–2):105–115.
57. Gan Q, Wang T, Cochrane C, McCarron P. Modulation of surface charge, particle size and morphological properties of chitosan-TPP nanoparticles intended for gene delivery. *Colloids Surf B Biointerfaces*. 2005;44(2–3):65–73. doi:10.1016/j.colsurfb.2005.06.001
58. Wang J, Zeng ZW, Xiao RZ, et al. Recent advances of chitosan nanoparticles as drug carriers. *Int J Nanomed*. 2011;6:765–774.
59. Rodrigues S, Dionísio M, López CR, Grenha A. Biocompatibility of chitosan carriers with application in drug delivery. *J Funct Biomater*. 2012;3(3):615–641. doi:10.3390/jfb3030615
60. Pandey R, Khuller GK. Chemotherapeutic potential of alginate-chitosan microspheres as anti-tubercular drug carriers. *J Antimicrob Chemother*. 2004;53:635–640. doi:10.1093/jac/dkh139
61. Sonaje K, Lin YH, Juang JH, Wey SP, Chen CT, Sung HW. In vivo evaluation of safety and efficacy of self-assembled nanoparticles for oral insulin delivery. *Biomaterials*. 2009;30:2329–2339. doi:10.1016/j.biomaterials.2008.12.066